HHS Public Access

Author manuscript

Toxicology. Author manuscript; available in PMC 2018 July 15.

Published in final edited form as:

Toxicology. 2017 July 15; 387: 81–94. doi:10.1016/j.tox.2017.05.018.

Deficiencies in mitochondrial dynamics sensitize *Caenorhabditis elegans* to arsenite and other mitochondrial toxicants by reducing mitochondrial adaptability

Anthony L. Luz[a], **Tewodros R. Godebo**[a], **Latasha L. Smith**[a], **Tess C. Leuthner**[a], **Laura L. Maurer**[b], and **Joel N. Meyer**[a,c]

[a]Nicholas School of the Environment, Box 90328, Duke University, Durham, NC, USA, 27708

[b]ExxonMobil Biomedical Sciences, Inc., Annandale, NJ, USA, 08801-3059

Abstract

Mitochondrial fission, fusion, and mitophagy are interlinked processes that regulate mitochondrial shape, number, and size, as well as metabolic activity and stress response. The fundamental importance of these processes is evident in the fact that mutations in fission (DRP1), fusion (MFN2, OPA1), and mitophagy (PINK1, PARK2) genes can cause human disease (collectively >1/10,000). Interestingly, however, the age of onset and severity of clinical manifestations varies greatly between patients with these diseases (even those harboring identical mutations), suggesting a role for environmental factors in the development and progression of certain mitochondrial diseases. Using the model organism *Caenorhabditis elegans,* we screened ten mitochondrial toxicants (2, 4-dinitrophenol, acetaldehyde, acrolein, aflatoxin B_1, arsenite, cadmium, cisplatin, doxycycline, paraquat, rotenone) for increased or decreased toxicity in fusion (*fzo-1, eat-3*)-, fission (*drp-1*)-, and mitophagy (*pdr-1, pink-1*)-deficient nematodes using a larval growth assay. In general, fusion-deficient nematodes were the most sensitive to toxicants, including aflatoxin B_1, arsenite, cisplatin, paraquat, and rotenone. Because arsenite was particularly potent in fission- and fusion-deficient nematodes, and hundreds of millions of people are chronically exposed to arsenic, we investigated the effects of these genetic deficiencies on arsenic toxicity in more depth. We found that deficiencies in fission and fusion sensitized nematodes to arsenite-induced lethality throughout aging. Furthermore, low-dose arsenite, which acted in a “mitohormetic” fashion by increasing mitochondrial function (in particular, basal and maximal oxygen consumption) in wild-type nematodes by a wide range of measures, exacerbated mitochondrial dysfunction in fusion-deficient nematodes. Analysis of multiple mechanistic changes suggested that disruption of pyruvate metabolism and Krebs cycle activity underlie the observed arsenite-induced

[c] joel.meyer@duke.edu.

Conflict of interest statement

The authors confirm that Laura L. Maurer completed their experimental contribution while employed at Duke University, and has since become employed at ExxonMobil Biomedical Sciences Inc. (EMBSI). EMBSI did not have any role in the study design, data collection and analysis, decision to publish, or preparation of the manuscript. All additional authors have no conflicts of interest to declare.

mitochondrial deficits, and these disruptions are exacerbated in the absence of mitochondrial fusion. This research demonstrates the importance of mitochondrial dynamics in limiting arsenite toxicity by permitting mitochondrial adaptability. It also suggests that individuals suffering from deficiencies in mitodynamic processes may be more susceptible to the mitochondrial toxicity of arsenic and other toxicants.

Keywords

Arsenite; gene-environment interaction; mitochondrial fission; mitochondrial fusion; mitophagy; mitochondrial toxicity

1. Introduction

Mitochondria, best known for their role in ATP production, are dynamic organelles that fuse and divide in response to various cellular and environmental cues. These cues regulate mitochondrial shape, number, and size, as well as the ability to meet demand for cellular energy (Chan 2012). Fission and fusion are mediated by guanosine triphosphatases in the dynamin family, whose combined action fuse and divide the mitochondrial double membrane. The process of fission is mediated by cytosolic dynamin-related protein-1 (DRP1), which is recruited to the outer mitochondrial membrane (OMM), forming a spiral that constricts upon GTP hydrolysis to drive scission of the organelle. Alternatively, membrane-anchored mitofusins (MFN1, MFN2) mediate fusion of the OMM, while OPA1 mediates fusion of the inner mitochondrial membrane (Chan 2006).

In addition to governing mitochondrial morphology, fission and fusion also play an important role in mitochondrial stress response (Youle and Van Der Bliek 2012). For example, mitochondria carrying low levels of damaged mitochondrial DNA (mtDNA) or proteins can fuse with healthy mitochondria allowing contents to mix, resulting in the generation of healthy mitochondria in a process known as functional complementation (Nakada et al. 2001; Schon and Gilkerson 2010). On the other hand, irreparably damaged mitochondria are hindered in rejoining the mitochondrial network through fusion, as a sustained loss of mitochondrial membrane potential triggers the proteolytic cleavage of OPA1 thus blocking inner membrane fusion, and preventing poisoning of the mitochondrial network (Head et al. 2009). Damaged mitochondria can then be eliminated via mitophagy, as loss of membrane potential also results in the accumulation of PTEN-induced putative kinase 1 (PINK1) on the OMM. PINK1 phosphorylates OMM proteins, including MFN2, and recruits the E3 ubiquitin ligase parkin (PARK2) from the cytosol. Parkin then ubiquitinates OMM proteins targeting the mitochondrion for autophagic degradation (Kim and Lemasters 2011; Twig et al. 2008). The importance of fission, fusion, and mitophagy (collectively referred to herein as “mitochondrial dynamics”) is demonstrated by the fact that deficiencies in these processes cause human disease. For example, mutations in *PINK1* and *PARK2* cause familial Parkinson’s Disease (PD) (Nuytemans et al. 2010), while mutations in *OPA1* and *MFN2* cause dominant optic atrophy (DOA) (Delettre et al. 2000) and Charcot-Marie-Tooth neuropathy type 2A (CMT2A) (Züchner et al. 2004), respectively. The population frequencies of pathological mutations of these genes are 1 in 10,000 – 50,000 for

OPA1 (Thiselton et al. 2001; Yu-Wai-Man et al. 2010), and 1 in 7,500 for *MFN2* (Cartoni and Martinou 2009; Feely et al. 2011). The frequency of *PINK1* and *PARK2* mutations is unknown; however, *PARK2* mutations account for up to 40% of early-onset PD cases (Vinish et al. 2010), while *PINK1* accounts for 5% (Bonifati et al. 2005). Mutations in *DRP1* are not commonly associated with disease, although a few reports of neurodegeneration and epilepsy have been published (Vanstone et al. 2015; Waterham et al. 2007).

Despite the clear importance of these gene mutations, only 10% of PD cases are linked to genetics (Klein and Westenberger 2012), while the age of onset and severity of clinical manifestations can vary dramatically between patients suffering from CMT2A, even in patients carrying identical mutations (Choi et al. 2015; Lv et al. 2015). These observations strongly suggest a role for the environment in the development and progression of certain mitochondrial diseases; however, the relationship remains poorly understood. To address this knowledge gap, we screened ten known and suspected mitochondrial toxicants (2,4-dinitrophenol (DNP), acetaldehyde, acrolein, aflatoxin B_1 (AfB_1), arsenite, cadmium, cisplatin, doxycycline, paraquat, rotenone) for exacerbation of mitochondrial dysfunction in fission (*drp-1*)-, fusion (*fzo-1, eat-3* (*MFN2*, *OPA1* homologs, respectively))-, and mitophagy (*pink-1*, *pdr-1* (*PINK1, PARK2* homologs, respectively))-deficient *Caenorhabditis elegans*. *C. elegans* is a powerful *in vivo* model to study mitochondrial gene-environment interactions, as mitochondrial function and many biochemical pathways are well conserved with humans (Maglioni and Ventura 2016; Murfitt et al. 1976; O'Riordan and Burnell 1989; Okimoto et al. 1992; Tsang and Lemire 2003; Zhang et al. 2013). *in vivo* analysis is important, as mitochondrial function is dependent upon intercellular signals, many of which arise from diverse tissues and cell types, and are lost in *in vitro* models (McBride et al. 2006).

Here, we identify several novel gene-environment interactions. In particular, deficiencies in fission and fusion sensitized nematodes to the inorganic trivalent arsenical, arsenite. Of the toxicants tested, arsenite may have the highest potential for human health relevance, as over 140 million people worldwide are chronically exposed to arsenite via consumption of contaminated drinking water (Chowdhury et al. 2006; Ravenscroft et al. 2009). Although chronic arsenite exposure is associated with cancer (Gilbert-Diamond et al. 2013; Karagas et al. 2004; Marshall et al. 2007; Yu et al. 2006), and other metabolism-related pathologies (Ditzel et al. 2015; Sanchez-Soria et al. 2014; Shi et al. 2013), the precise mechanisms underlying pathogenesis are complex, and remain poorly understood. We also demonstrate that arsenite disrupts mitochondrial energy metabolism in fusion (*fzo-1*, *eat-3*)-deficient nematodes, while increasing mitochondrial function in wild-type nematodes, and has minimal effect on mitochondrial function in fission (*drp-1*)-deficient nematodes. These results support the importance of mitochondrial disruption in arsenic's mechanism of toxicity, highlight the critical role for mitochondrial dynamics in responding to exposure, and suggest that a significant fraction of the population may be especially vulnerable to arsenic toxicity due to genetic deficiencies in mitochondrial dynamics.

2. Methods

2.1 *C. elegans* strains and culture conditions

Wild-type (N2 Bristol), VC1024 *pdr-1* (*gk448*; outcrossed (OC) × 3), and SJ4103 (zcIs14 [*myo-3*::GFP (mit)]) nematodes were purchased from the *Caenorhabditis* Genetics Center (CGC, University of Minnesota). CU5991 *fzo-1* (*tm1133*; OC × 4) and DA631 *eat-3* (*ad426*; OC >1) were provided by Alexander Van der Bliek, University of California, CU6806 *fzo-1* (*tm1133*); *drp-1* (*tm1108*) and CU6372 *drp-1* (*tm1108*; OC × 9) were provided by Ding Xue, University of Colorado, and *pink-1* (*tm1779*; OC × 1) were provided by Guy Caldwell, University of Alabama. All strains are referred to elsewhere in this manuscript by their gene name.

Synchronous populations of larval stage 1 (L1) nematodes were generated via sodium hydroxide bleach treatment as previously described (Lewis and Fleming 1995), followed by overnight incubation on an orbital shaker in complete K-medium (150µl 1M $CaCl_2$, 150µl 1M $MgSO_4$, 25µl 10mg/ml cholesterol, 50mL sterile K medium (2.36g KCl, 3g NaCl, 1L ddH_2O)) at 20°C. Synchronous populations of nematodes were then maintained on K-agar plates seeded with *Escherichia coli* OP50 at 20°C as previously described (Stiernagle 1999).

2.2 Larval growth

Larval growth was measured using the COPAS Biosort (Union Biometrica Inc., Somerville, MA) as previously described (Boyd et al. 2010). Fifty L1 nematodes were loaded into each well of a 96-well plate (4–6 wells per strain per treatment) using the COPAS Biosort. The volume of each well was then brought to 100µl with EPA H_2O (Weber 1991), UVC-killed UvrA (UVC sensitive *E. coli* strain due to a lack of nucleotide excision repair (Croteau et al. 2008)), and toxicant. With the exception of sodium arsenite (Ricca Chemical Company), all chemicals were purchased from Sigma-Aldrich (St. Louis, MO). L1 nematodes were exposed to DNP (0, 250, 500, 1000µM in 0.5% DMSO), acetaldehyde (0, 1, 5mM in ddH_2O), acrolein (0, 150, 200, 250, 300µM in ddH_2O), AfB_1 (0, 1, 3, 10µM in 0.5% DMSO), arsenite (0, 400, 600, 800µM in ddH_2O), cadmium chloride (0, 20, 80, 150µM in ddH_2O), doxycycline (0, 2.5, 5, 7.5µg/ml in 0.5% DMSO), paraquat dichloride hydrate (0, 25, 50, 150µM in ddH_2O), rotenone (0, 250, 500, 750nM in 0.5% DMSO) or cisplatin (0, 10, 20, 40, 60µM in ddH_2O). Caution must be used when handling acetaldehyde and acrolein, as these compounds are highly volatile. In addition 2,4-DNP is highly ionized at neural pHs (based on a pK_a of 4.11); thus, reducing pH of the dosing media may increase the potency of DNP, as unionized compounds penetrate the cuticle more efficiently. Nematodes were allowed to develop at 20°C for 48h, and larval growth was determined using the COPAS Biosort (Boyd et al. 2010). All time of flight (ToF) data, a surrogate for nematode length, was normalized to percent control for each strain prior to statistical analysis, as some of the strains develop at reduced rates compared to wild-type nematodes under control conditions. Cisplatin growth assays were performed using a combination of the COPAS Biosort and Fiji-based measurements of nematode images acquired using NIS-Elements BR software and a Nikon SMZ1500 stereomicroscope. Nematode length was measured in Fiji using the segmented line function with splice fitting. All experiments were repeated 2–3 separate times.

2.3 Reproduction

Nematode reproduction was determined as previously described (Boyd et al. 2010). Briefly, three L4 nematodes were loaded into each well of a 96-well plate (4–6 wells per strain per treatment) using a COPAS Biosort (Union Biometrica Inc., Somerville, MA). The final volume of each well was then brought to 100µl with EPA water, UV-killed UvrA, and arsenite to a final concentration of 0, 200, 400, or 600µM. Nematodes were then allowed to reproduce for 48h at 20°C, and progeny were counted using the COPAS Biosort. Data was normalized to percent control, as some strains lay eggs at a reduced rate and/or have reduced fecundity compared to wild-type nematodes. Experiments were repeated three separate times.

2.4 Lethality and rescue assays

Arsenite lethality assays—Ten L4, 8 or 12 day old N2, *fzo-1*, *eat-3*, and *drp-1* nematodes were added to each well of a 96-well plate using a platinum worm pick (2 wells per treatment per strain). The volume of each well was then brought to 100µl with complete k-medium, UV-killed UvrA, and arsenite to a final concentration of 0, 50, 100, 250, 500, 750, 1000, 1500, 2000, 3000, 4000, or 5000µM. Nematodes were exposed to arsenite for 24h at 20°C, and then scored as dead if they failed to move after repeated probing with a platinum worm pick.

Antioxidant and 3-MA rescue assays—Nematodes were exposed to antioxidants or small molecule inhibitors at concentrations previously shown to have therapeutic effects in nematodes (Ahn et al. 2014; Bess et al. 2012; Ng et al. 2014). Briefly, ten 7.5-day old nematodes were added to each well of a 96-well plate and exposed to 10mM 3-MA, 100µM deferoxamine, 40µM trolox, 60µM N- acetyl cysteine, or 5µM mitoQ for 12 hours. Each strain was then exposed to its 24h LC_{50} concentration of arsenite, and lethality was scored 24h later.

Dichloroacetate rescue—L1 stage nematodes were placed on k-agar plates containing 500µM DCA, a concentration that has previously been shown to increase steady-state ATP levels in nematodes (Schaffer et al. 2011), and allowed to develop at 20°C to the L4 stage. Nematodes were then exposed to 0, 2, 3, or 6 mM arsenite in liquid (as described above), and scored for survival 24 hours later.

Basal OCR rescues—7.5-day old nematodes were exposed to 5µM mitoQ or 10mM 3-MA for 12 hours, and then exposed to 100µM arsenite for 24h. Following arsenite exposure, basal OCR was measured using the Seahorse XF^e24 Bioanalyzer as described in section 4.6.

Secondary toxicant exposures—Following 24h exposure to 100µM arsenite, nematodes were exposed to secondary heat (37°C) or redox stress (100mM paraquat). Briefly, 10 nematodes were placed on a k-agar plate using a platinum worm pick and placed in a 37°C incubator. Nematodes were scored (every 2 hours) as dead when they failed to move after repeated probing with a platinum worm pick. The paraquat lethality assay was scored once, after 24h liquid exposure to paraquat.

2.5 Lifespan

Nematode lifespan was determined following chronic, lifelong (initiated at L1) exposure to 0, 25, or 100μM arsenite, and after acute (24h) exposure to 100uM arsenite in 8 day old nematodes. Twenty-five nematodes were added to control or arsenite containing K-agar plates seeded with *E. coli* OP50 and allowed to develop. Nematodes were monitored daily, and were scored as dead when they failed to move in response to repeated probing with a platinum worm pick. Lifespan experiments were repeated 2–3 separate times.

2.6 Seahorse XF^e analysis

Using the Seahorse XF^{e}24 Extracellular Flux Analyzer (Seahorse Bioscience, Massachusetts, USA), basal oxygen consumption rate (OCR), maximal OCR, and spare respiratory capacity were measured as previously described (Luz et al. 2015a; Luz et al. 2015b). Briefly, nematodes were resuspended in unbuffered EPA H_2O to a final concentration of 1.0±0.2 nematodes per microliter. Forty to seventy-five (75 L4 vs. 40 eight- and twelve-day old) nematodes were then pipetted into each well of a Seahorse utility plate, and the final volume of each well was brought to 525μl with unbuffered EPA H_2O. An aliquot of nematodes was then frozen for total protein determination via the bicinchoninic acid assay (ThermoFisher Scientific). Eight basal OCR measurements were taken prior to the injection of 25μM FCCP (mitochondrial uncoupler), and then an additional 8 OCR measurements were taken following FCCP injection. Seahorse experiments were repeated three separate times.

2.7 ATP determination

Relative steady-state ATP levels were determined as previously described (Bailey et al. 2016). First, 200 L4, 50 8-day old, or 50 12-day old nematodes were loaded into a white 96-well plate (3 wells per strain per treatment) in 50μl k-medium, and then 50μl of Promega Mitochondrial ToxGlo assay medium (Promega, Madison, WI) was added to each well. Nematodes were then incubated at 20°C for 30 minutes, and then luminescence was measured using a FLUOstar Optima microplate reader equipped with a luminescence optic. Experiments were repeated 3–5 separate times.

2.8 Genome copy number determination

Mitochondrial (mtDNA) and nuclear (nucDNA) genome copy number were determined as previously described (Gonzalez – Hunt et al. 2016; Rooney et al. 2015). Briefly, 6 nematodes were added to 90μl proteinase K-containing lysis buffer using a platinum worm pick and frozen at −80°C. Samples were then thawed, and lysed by heating to 65°C for 1h. Crude nematode lysate was used as template DNA for RT-PCR based determination of mtDNA and nucDNA copy number. Standard curves were employed for determination of absolute copy number. Three samples per treatment per time point were collected for each experiment. Experiments were repeated 2 separate times.

2.9 Isolation of mitochondria and nematode lysate

Following arsenite exposure, nematodes were rinsed 2 times with cold MSM buffer (20.04g mannitol, 11.98g sucrose, 523.5mg MOPS, 0.5L milliQ H_2O, pH 7.4), transferred to a glass

homogenizer and homogenized for 3 minutes. The homogenate was then transferred to an ultracentrifuge tube and spun at 300 × G for 10min at 4°C. The supernatant was then transferred to new tube and spun at 7000 × G for 10min at 4°C to yield the mitochondrial pellet. The supernatant was then discarded, and the pellet was resuspended in MSM buffer, and re-pelleted two additional times to rinse the mitochondrial fraction.

Following arsenite exposure, nematodes were rinsed two times with cold MSM buffer, transferred to a glass homogenizer and homogenized for 2min. The homogenate was then transferred to an ultracentrifuge tube and spun at 300 × G for 5min at 4°C to remove excess cuticle and large debris. The supernatant was then transferred to a new tube and spun at an additional two times to yield the crude nematode lysate.

2.10 Enzyme activity

Citrate synthase activity was measured in crude nematode lysate as detailed in (Srere 1969; Trounce et al. 1996). Briefly, CHAPs (1% final concentration) was added to the crude lysate and allowed to sit on ice for 15min to solubilize the inner mitochondrial membrane. Samples were then spun at 14,000 RPM for 10min, and the resulting supernatant was used for measuring citrate synthase activity. 10µl (20–40µg protein) of the homogenate, 2µl 30mM acetyl-CoA, 2µl 10mM DTNM, and 176µl 100mM Tris HCl (pH 8) was pipetted into a clear 96 well plate, and allowed to sit at 25°C for 10min to initiate the reaction. Absorbance at 412nm was then measured every 20s for 3 minutes using a FLUOstar Optima microplate reader to measure the endogenous DTNM reduction. 10µl 10mM oxaloacetate was then added to each sample and absorbance at 412nm was measured every 20s for 5min. The change in absorbance over the linear range was calculated with endogenous DTNM reduction subtracted, and then normalized to total protein.

ETC CI activity was assayed in isolated mitochondria as previously described (Estornell et al. 1993). Briefly, mitochondria were incubated in 20mM potassium phosphate buffer, 2.5mg/ml fatty-acid free BSA, and 2mM KCN at 20°C for 10min. 2.0µl 5mM NADH and 2.0µl 2.5mM coenzyme Q_1 were then added to each well, and the rate NADH oxidation (Abs_{340nm}) was measured using a microplate reader. 40µM Rotenone was then added to each well to measure non-specific NADH oxidation.

Pyruvate and isocitrate dehydrogenase activity (PDH and IDH, respectively) were measured in isolated mitochondria following 24h of exposure to 100µM arsenite using Colorimetric Assay Kits (BioVision, Cat. # K679 and K756). Mitochondria were isolated as described above, and resuspended in BioVision's PDH or IDH Assay Buffer. PDH and IDH activity was then measured following the manufacturer's instructions. All experiments were repeated 3 separate times.

2.11 Glycolysis assay

Glycolysis was assayed as described in (Luz et al. 2016b). Briefly, 50 control or arsenite exposed nematodes were pipetted into each well (3 wells per treatment) of a white 96-well plate and exposed to EPA H_2O or 50mM 2-DG (final volume 50µl) for 4.5h at 20°C. 50µl of Promega Mitochondrial ToxGlo assay medium was then added to each well and steady-state ATP was determined as described in Section 2.7.

2.12 Gene expression

mRNA was isolated from nematodes using the Qiagen RNeasy Mini kit. 1500ng mRNA was then converted to cDNA using the Qiagen Omniscript Reverse Transcription kit. mRNA levels from control and arsenite treated nematodes were then measured using the 7300 Real-time PCR System. Table S1 lists the annealing temperatures, amplicon sizes, and sequences of all PCR primers. The fold change of each gene was then calculated by comparing the cycle threshold (C_t) of the target gene to the C_t of the house keeping gene *cdc-42* (Hoogewijs et al. 2008). Samples were collected in triplicate from two independent experiments.

2.13 Mitochondrial morphology

Control and arsenite exposed nematodes were exposed to 1μM Mitotracker Red CMXROS (Molecular Probes, Invitrogen) in complete K-medium overnight. Following Mitrotracker exposure, nematodes were rinsed 2 times in fresh K-medium and incubated on an orbital shaker at 20°C for 30 minutes to allow excess dye to clear from their guts. Nematodes were then picked onto an agar pad containing levamisole (25 mg/mL) and subsequently imaged on a confocal microscope (Zeiss Axio 780 confocal upright with fixed stage) (Luz et al. 2015a).

2.14 Arsenite analysis

Internal concentrations of arsenic were measured in isolated mitochondria and in the crude nematode lysate. Briefly, following isolation, samples were treated with concentrated HNO_3 acid (1.5 ml, 15 N), 0.5 ml of ddH2O, and 5 drops of 30% H_2O_2. The samples were then heated progressively on a hotplate from 50 to 80°C for 12h, while regularly being degassed (after 30min cooling) until the digestion step was completed. 0.45ml aliquots of the digested samples were then analyzed for total arsenic via a VG Plasmaquad 3 inductively coupled plasma–mass spectrometer.

2.15 Statistical analysis

Statistical analysis was performed using JMP v11.0 software (SAS Institute). LC_{50} values were calculated using Probit analysis. Survival curves were analyzed via the non-parametric Mantel cox test. All other data was initially assessed via one or two way ANOVA, and when warranted ($p<0.05$) post-hoc analysis was performed using Tukey's HSD test.

3. Results

3.1 Deficiencies in mitochondrial dynamics generally sensitize, but in some cases protect, nematodes from environmental mitotoxicants

We wished to test whether deficiency in mitodynamic processes would sensitize nematodes to exposure to chemicals that cause mitochondrial damage. As larval development is dependent upon proper mitochondrial function in nematodes (Rea et al. 2007; Tsang et al. 2001), we tested ten known and suspected mitotoxicants (DNP, acetaldehyde, acrolein, AfB_1, arsenite, cadmium, cisplatin, doxycycline, paraquat, and rotenone) for exacerbation of larval growth delay in fission (*drp-1*)-, fusion (*fzo-1*, *eat-3*)-, and mitophagy (*pdr-1*, *pink-1*)-

deficient nematodes using a COPAS Biosort-based larval growth assay (Anderson et al. 2001; Boyd et al. 2010). Results from the larval growth screen are presented in a condensed form in Table 1 to facilitate examination of general patterns of toxicant-genotype interaction; however, this presentation decreases the actual magnitude of the biological effects observed, and obscures details of the individual dose-responses for each strain. Therefore, the full dose-responses after exposure to each chemical are presented in Figure 1 and Figures S1–S10.

Deficiencies in mitochondrial fusion genes *fzo-1* and *eat-3* sensitized nematodes to arsenite (Fig 1A and Fig S1), AfB_1 (Fig S2), paraquat (Fig S3), rotenone (Fig S4), DNP (Fig S5), and cisplatin (Fig S6), while only mildly sensitizing nematodes to acetaldehyde (Fig S7). Alternatively, deficiencies in mitochondrial fission (*drp-1*) only mildly sensitized nematodes to paraquat (Fig S3). Interestingly, deficiencies in *pink-1* and *pdr-1* resulted in varied responses to toxicants. *pdr-1*-deficient nematodes were mildly sensitized to rotenone (Fig S4), while *pink-1* nematodes were sensitive to rotenone (Fig S4), and mildly sensitive to DNP (Fig S5), and doxycycline (Fig S10). Unexpectedly, resistance to several toxicants was observed. All fission-, fusion-, and mitophagy-deficient strains displayed resistance to acrolein (Fig S8), while only *fzo-1* nematodes displayed resistance to cadmium (Fig S9), and *pink-1* was mildly resistant to acetaldehyde (Fig S7).

Of the mitotoxicants tested, arsenite stood out as causing a large differential effect in multiple mitodynamics strains compared to wild-type. Furthermore, the highest concentration of arsenite tested (800μM) induced significant lethality in *fzo-1* and *eat-3*, but not in other nematode strains. In addition, arsenic is of immense human health concern, as demonstrated both by the large number of people who are exposed due to drinking water contamination (described above), and by its importance at highly polluted sites around the United States (it was listed first on the Agency for Toxic Substances and Disease Registry's 2015 substance priority list). Thus, arsenite was chosen for further mechanistic studies.

3.2 Deficiencies in mitochondrial fission and fusion sensitize nematodes to arsenite throughout aging

We hypothesized that fission and mitophagy deficiencies, which surprisingly did not result in sensitivity during our short-term larval growth assay, would be more deleterious over a longer time-course, as lack of these processes would inhibit removal of damaged mitochondria. To test this, we exposed L4 stage *drp-1, pink-1,* and *pdr-1* nematodes to arsenite and monitored reproduction. Deficiencies in *drp-1*, but not *pdr-1* or *pink-1* sensitized nematodes to arsenite-induced reproductive toxicity (Fig 1B). We therefore included *drp-1*, but not *pdr-1* or *pink-1* in subsequent studies.

Next, to identify non-lethal arsenite exposure conditions and potential windows of sensitivity throughout aging, we performed acute and chronic arsenite exposures with young (L1–L4 stage), middle (8-day old) and old age (12-day old) nematodes. Chronic, lifelong exposure to 25μM arsenite did not affect nematode lifespan, while 100μM arsenite reduced the lifespan of all strains; however *fzo-1, eat-3,* and *drp-1* were not significantly sensitive compared to wild-type (Table S2 and Fig S11). On the other hand, *fzo-1* and *eat-3* were hypersensitive to acute arsenite toxicity (24h lethality) throughout aging (L4, 8-, 12-days of

age), while *drp-1* were sensitive only later in life (8- and 12-days of age) compared wild-type nematodes (Fig 2A–C). Sensitivity to arsenite-induced lethality increased dramatically (more than 10-fold) throughout aging in all strains, with 24h LC_{50} values declining from 5.73 (N2), 2.76 (*fzo-1*), 2.97 (*eat-3*), 6.03 (*drp-1*) mM arsenite at the L4 stage to 0.64 (N2), 0.22 (*fzo-1*), 0.12 (*eat-3*), 0.38 (*drp-1*) mM arsenite at 12-days of age (Table 2). This age-related increase in sensitivity to arsenite may be due to a concurrent age-related decline in DNA repair capacity (Meyer et al. 2007), antioxidant defenses (Brys et al. 2007), or other homeostatic processes in aging *C. elegans*.

3.3 Arsenite preferentially disrupts mitochondrial function in fusion-deficient nematodes throughout aging

While previous research and our results up to this point provides evidence that arsenite targets mitochondria, they do not specifically demonstrate altered mitochondrial function, or strain-specific differences in the mitochondrial response to arsenic. Therefore, we next investigated the effects of non-lethal arsenite exposure (25, 100, or 1,500μM depending upon life stage) on mitochondrial function in L4 stage, 8- and 12-day old *fzo-1, eat-3, drp-1*, and wild-type nematodes. Of note, and as described below, these concentrations of arsenic result in internal concentrations of arsenic comparable to those observed in people exposed to high levels of arsenic in drinking water (Section 4.2). Arsenite reduced basal OCR and ATP content in L4 stage *fzo-1* and *eat-3* nematodes, while also reducing spare respiratory capacity (SRC) in N2, *fzo-1*, and *eat-3* nematodes (Fig 3A–D). Unexpectedly, arsenite increased basal OCR, maximal OCR, and spare respiratory capacity (trending increase, P=0.059 for post-hoc comparison) in 8-day old wild-type nematodes (Fig 3E–H), while reducing basal OCR, ATP, maximal OCR, and SRC in fusion (*fzo-1, eat*)-deficient nematodes (Fig 3E–H). Finally, at 12-days of age arsenite increased basal OCR in wild-type nematodes, decreased basal OCR in *eat-3* and *drp-1,* had no effect on ATP or maximal OCR, and decreased SRC in *fzo-1* (Fig 3I–L). However, maximal OCR and SRC declined steadily throughout aging until SRC fell below detection limits in 12-day old *eat-3* and *drp-1* nematodes (Fig 3L); thus, these parameters must be interpreted with caution in aging nematodes. Interestingly, the mitochondrial response to arsenite was not identical for fusion-deficient *fzo-1* and *eat-3* nematodes (Fig 3A, E, I); however, it is important to note that these genes have additional roles beyond mitochondrial fusion. For example, *fzo-1* plays a role in crosstalk between mitochondria and the endoplasmic reticulum (Sugiura et al. 2013), while *eat-3* plays a role in mitochondrial cristae formation and mtDNA stability (Elachouri et al. 2011). These alternative functions may underlie the fact that mutations in MFN2 and OPA1 cause different human diseases (CMT2A vs. DOA); thus, identical responses to arsenite would be unexpected. P-values for statistical analysis are provided in Table S3.

Collectively, these results demonstrate that arsenic disrupted mitochondrial function in fusion-deficient nematodes, while having minimal adverse effects or even beneficial effects on mitochondrial function in wild-type and *drp-1* nematodes. The lack of effect in *drp-1* nematodes is particularly remarkable given their reduced basal SRC. Furthermore, these results also demonstrate an age-related increase in sensitivity to arsenite-induced mitochondrial dysfunction in fusion-deficient nematodes.

3.4 The role of mitochondrial morphology, autophagy, ROS, the unfolded protein response, and mitochondrial biogenesis in arsenite-induced toxicity

Mitochondrial dynamics are integral to many homeostatic processes. To investigate which were responsible for the sensitivity of the fusion-deficient strains, we next investigated the role of mitochondrial morphology, autophagy, reactive oxygen species (ROS), the unfolded protein response (UPR), and mitochondrial biogenesis in arsenite-induced mitochondrial dysfunction. Because development of the nematode germline at the L3–L4 transition is associated with large increases in mtDNA copy number and oxidative phosphorylation (OXPHOS) (Tsang and Lemire 2002; Tsang and Lemire 2003), which would confound mechanistic studies, we performed all experiments in post-mitotic, 8-day old nematodes, using a non-lethal 24h exposure to 100μM arsenite. This life stage was also of particular interest because arsenite exposure at 8 days induced opposing responses in wild-type and fusion-deficient nematodes, enhancing mitochondrial function in wild-type and disrupting mitochondrial function in fusion-deficient nematodes (Fig 3E–H).

3.4.1 Mitochondrial morphology per se does not influence arsenite sensitivity—Because mitochondrial fusion facilitates functional complementation, we hypothesized that arsenite would induce mitochondrial fusion in wild-type nematodes. This would be consistent with fusion deficiency conferring sensitivity, since *fzo-1* and *eat-3* nematodes would lack this protective response. Moreover, hyper-fused mitochondria tend to be more metabolically active (Pich et al. 2005; Westermann 2012); thus an increase in mitochondrial fusion could also explain the increase in mitochondrial respiration observed in wild-type nematodes. However, arsenite had no detectable effect on mitochondrial morphology (representative images shown in Fig S12) or expression of *drp-1* or *fzo-1* mRNA in wild-type nematodes (Fig S13), expression of which has previously been shown to track well with toxicant-induced alterations in mitochondrial morphology (Li et al. 2015). Next, as mitochondrial morphology is maintained through a balance of fission and fusion, and loss of both fission and fusion restores mitochondrial networks back to a wild-type morphology (Breckenridge et al. 2008), we hypothesized that inhibition of *drp-1* in *fzo-1* or *eat-3* nematodes would reduce sensitivity to arsenite. Pharmacological inhibition of *drp-1* with mdivi-1 (Cassidy-Stone et al. 2008; Whelan et al. 2012) in *fzo-1* and *eat-3* nematodes had no effect on mitochondrial morphology in either strain (data not shown). Finally, we tested L4 stage *fzo-1; drp-1* double mutants for sensitivity to arsenite using a 24h lethality assay; however, *fzo-1; drp-1* double mutants displayed similar sensitivity to arsenite as *fzo-1* nematodes (Fig S14). Collectively, these results demonstrate that mitochondrial morphology alone does not dictate arsenite sensitivity, but are consistent with the importance of being capable of mounting a dynamic morphological response to stress (which is lost in the double mutant).

3.4.2 Autophagy has a limited role in arsenite toxicity—Autophagy is often a protective response, but can in some cases cause toxicity. In response to starvation-induced autophagy, mitochondria upregulate fusion to elongate the mitochondrial network. Because elongated mitochondria are recalcitrant to autophagic degradation (Rambold et al. 2011), increased fusion may represent a protective response that maintains mitochondrial mass, which would be lost in *fzo-1* and *eat-3* nematodes. As arsenite can induce autophagy in *C.*

elegans (Luz et al. 2016a) and other mammalian models (Bolt et al. 2010; Zhang et al. 2012), we hypothesized that arsenite-induced autophagy results in degradation of fragmented mitochondria in fusion-deficient nematodes resulting in reduced mitochondrial content and dysfunction. In partial agreement with this, pretreating *fzo-1*-deficient nematodes with the type III phosphatidylinositol 3-kinase inhibitor 3-methyladenine (3-MA) partially rescued nematodes from arsenite-induced lethality (Fig S15); however, 3-MA pretreatment failed to prevent low-dose (100μM) arsenite from reducing basal OCR in fusion-deficient nematodes (Fig S15). Furthermore, 100μM arsenite did not induce autophagy (*lgg-1*, *atg-18*) or mitophagy (*dct-1*) gene expression (Fig S16). Collectively, these results suggest that arsenite-induced autophagy may exacerbate lethality in *fzo-1* at higher, acutely toxic concentrations; however, at lower, non-lethal concentrations, autophagy does not appear to play a role in inducing mitochondrial dysfunction.

3.4.3 Arsenite induces superoxide dismutase expression—Generation of ROS is thought to be one of the principal mechanisms by which arsenic induces disease (Shi et al. 2004). As arsenite has been shown to induce ROS in *C. elegans* (Luz et al. 2016a; Sahu et al. 2013), and as deficiencies in *eat-3* have been shown to sensitize nematodes to ROS (Kanazawa et al. 2008), we hypothesized that arsenite-induced ROS was contributing to the mitochondrial dysfunction observed in fusion-deficient nematodes. However, treatment with N-acetyl cysteine, trolox (a water-soluble vitamin E analog), or deferoxamine (iron chelator that limits Fenton chemistry) failed to alter sensitivity to arsenite-induced lethality in any strains (Fig S17). On the other hand, treatment with the mitochondrial-targeted antioxidant mitoQ partially rescued lethality in *eat-3* and *drp-1* (Fig S18); however, mitoQ increased basal OCR in fission- and fusion-deficient nematodes regardless of arsenite treatment, confounding interpretation of results from an attempted mitoQ rescue of basal OCR (Fig S18). Next, to gain insight into the specific intracellular compartments where superoxide is being generated we measured expression of cytosolic (*sod-1*), mitochondrial (*sod-2, sod-3*), and extracellular (*sod-4*) superoxide dismutase genes. Treatment with 100μM arsenite induced *sod-1* in wild-type, *fzo-1*, and *eat-3*; had no effect on *sod-2* expression; decreased *sod-3* expression in wild-type and *fzo-1*; and increased *sod-4* expression in *fzo-1* nematodes (Fig S19). As expected, these results suggest a role for superoxide anion in arsenite toxicity; however, they are not supportive of mitochondria being the principle site of superoxide-generation.

3.4.4 Arsenite induces the unfolded protein response and disrupts pyruvate metabolism, with exacerbation of mitochondrial dysfunction specifically in fusion mutants—The binding of protein sulfhydryl groups by arsenite is one of the principal mechanisms of toxicity of arsenite, resulting in enzyme inhibition and protein misfolding. An induction of the UPR can serve to counteract this toxicity, but can also contribute to arsenite-induced toxicity and pathogenesis (Kitchin and Wallace 2008; Sahu et al. 2013). To test the potential protective or pathological roles of the UPR in this context, we next measured cytosolic (*hsp-16.2*), endoplasmic reticulum (*hsp-4*), and mitochondrial (*hsp-6*) specific heat shock protein (HSP) expression. Arsenite induced *hsp-16.2* in all strains, but *hsp-4* only in *fzo-1*, and *hsp-6* only in *fzo-1* and *eat-3* (Fig 4A–C). These results

confirm arsenite induces the UPR in *C. elegans*, and suggest a disruption specifically of mitochondrial proteostasis occurs at this level of exposure only in *fzo-1* and *eat-3*.

To test whether specific disruption of mitochondrial enzymes is also more sensitive in fusion mutants, we compared inhibition of known targets of arsenite across strains. Arsenite inhibits enzymes involved in pyruvate metabolism and the Krebs cycle, including pyruvate, succinate, isocitrate, and α-ketoglutarate dehydrogenases (Bergquist et al. 2009; Higashi et al. 1965; Hosseini et al. 2013; Luz et al. 2016a). We measured the activity of pyruvate (PDH) and isocitrate dehydrogenase (IDH); activity of both was inhibited by arsenite in *fzo-1* and *eat-3* (Fig 5A–B), but not in *drp-1* or wild-type nematodes. As compensatory shifts in metabolism from OXPHOS to aerobic glycolysis have been reported following arsenite exposure (Luz et al. 2016a; Zhao et al. 2013), we next tested for sensitivity to the hexokinase inhibitor 2-deoxy-D-glucose (2-DG) and measured glyceraldehyde 3-phosphate dehydrogenase expression (*gpd-3,* catalyzes the 6th step of glycolysis), which has previously been shown to be an inducible marker of glycolysis in nematodes (Zuryn et al. 2010). Arsenite exposure did not sensitize any strain to 2-DG-induced reductions in steady-state ATP levels (Fig S20), nor did arsenite alter *gpd-3* mRNA expression in fission- or fusion-deficient nematodes (Fig S20). However, a reduction in *gpd-3* expression was observed in wild-type nematodes. Collectively, these results suggest that disruption of pyruvate metabolism and Krebs cycle activity underlie arsenite-induced mitochondrial dysfunction in *fzo-1* and *eat-3* nematodes.

3.4.5 Cellular and organismal excretion of arsenic—As extrusion of arsenite via the ArsA ATPase (*asna-1*) is one mechanism by which nematodes detoxify arsenic (Tseng et al. 2007), we hypothesized that reduced mitochondrial function in fission- and fusion-deficient nematodes may limit arsenite excretion in these metabolically compromised strains. In partial agreement with this, arsenite accumulated in crude nematode lysate isolated from *drp-1*, but not *fzo-1* or *eat-3*, compared to wild-type nematodes (Fig S21); however, arsenite did not differentially accumulate in isolated mitochondria (Fig S21), nor did arsenite exposure significantly affect *asna-1* expression (Fig S22). To further test the role of energetics in limiting arsenite excretion we treated nematodes with the PDH kinase (a negative regulator of PDH) inhibitor dichloroacetate (DCA), which has previously been shown to increase steady-state ATP levels and reduce lactic acidosis in wild-type and *fzo-1* nematodes, respectively (Johnson and Nehrke 2010; Schaffer et al. 2011). In agreement with previous reports, DCA treatment increased steady-state ATP levels (Fig S22); however, DCA treatment failed to reduce sensitivity to arsenite-induced lethality in any strain (Fig S22). These results suggest that steady-state ATP levels are not rate limiting in the excretion of arsenite by the ArsA ATPase in nematodes. A limitation to interpreting these results is that it is unclear if DCA treatment can overcome PDH inhibition by arsenite in fusion-deficient nematode strains, although PDH inhibition was not observed in wild-type nematodes.

3.4.6 Arsenite increases mitochondrial function in wild-type nematodes—Unexpectedly, arsenite increased mitochondrial function in 8-day old wild-type (but not mutant) nematodes (Fig 3E–H). This could not be attributed to mitochondrial fusion, a process associated with increased metabolic activity, since no increase in mitochondrial

fusion was observed (Fig S12 & Fig S13). To test the alternate hypothesis that increased oxygen consumption resulted from mitochondrial biogenesis, we measured the expression of mitochondrial DNA polymerase γ (*polg-1*, the sole replicative mitochondrial DNA polymerase), the *C. elegans* mitochondrial transcription factor A (*TFAM*) ortholog (*hmg-5*), which is required for mtDNA replication and transcription (Sumitani et al. 2011), and mtDNA encoded *nd-5* (ETC CI) and *ctb-1* (ETC CIII). However, arsenite did not significantly alter the expression of *polg-1* or *hmg-5* in any strain (Fig S23). Arsenite did induce a small, but significant increase in *nd-5* expression in *eat-3*, while mildly reducing *ctb-1* expression in wild-type nematodes (Fig S23). As a clear transcriptional response for biogenesis was not observed, we next quantified mitochondrial mass in body wall muscle cells using transgenic nematodes expressing mitochondrial-targeted GFP under the control of the body wall muscle specific promoter *myo-3*. Arsenite did not increase GFP expression in body wall muscle cells (Fig S24). However, it is not clear whether GFP expression would be induced via the *myo-3* promoter in the context of biogenesis; it is possible that instead the same amount of GFP may simply diffuse into more mitochondria resulting in no net change of GFP expression. Therefore, we next measured whole worm citrate synthase (CS) activity, a frequently used biomarker of mitochondrial content (Larsen et al. 2012), and observed a large (~45%) increase in CS activity in wild-type, but not mutant, nematodes following arsenite exposure (Fig 6A). Furthermore, arsenite increased ETC CI activity in wild-type nematodes (Fig 6B); while a non-significant trend in increased mtDNA content was also observed (Fig 6C). Collectively, these results confirm that arsenite enhances mitochondrial function in wild-type nematodes, but not fusion-deficient strains. However, this effect either may occur without an increase in mitochondrial biogenesis and mass, or may be limited to specific tissues, as no increase in body wall muscle GFP was observed.

3.4.7 Increased respiration associated with decreased, not increased, stress resistance—Exposure to low-dose (100nM) arsenite has previously been shown to extend nematode lifespan, increase stress resistance, increase mitochondrial respiration, and upregulate mitochondrial protein content (Schmeisser et al. 2013), a phenomenon termed mitohormesis. However, the arsenite-induced increase in mitochondrial function in wild-type nematodes in the current study (which employs a higher exposure level) does not appear to represent a hormetic response, as no increase in lifespan was observed in any strain (Fig S25 & Table S4), nor did arsenite exposure increase stress resistance. Instead, arsenite sensitized fission, fusion, and wild-type nematodes to the free radical generator paraquat (Fig 7A), and *eat-3* and *drp-1* deficient nematodes to thermal stress (Fig 7B). Furthermore, the observed enhancement of mitochondrial function is no longer apparent after longer (48h) arsenite exposures in wild-type nematodes (Fig S26). Instead, early signs of mitochondrial dysfunction (reduced maximal OCR, and trending reduction in SRC) begin to become apparent after longer arsenite exposures.

4. Discussion and Conclusions

4.1 Gene-environment interactions between mitochondrial dynamics genes and mitotoxicants are complex

We initially hypothesized that deficiencies in mitochondrial dynamics, processes critical for mitochondrial function and stress response, would universally sensitize nematodes to toxicants that target mitochondria. While we did uncover strong, novel gene-environment interactions, the nature of those interactions was complex. Mitochondrial fusion (*fzo-1, eat-3*)-deficient nematodes were hyper-sensitive to the most toxicants, while mitophagy- and fission-deficient nematodes were sensitive to fewer toxicants, and in most cases where sensitivity was observed, the sensitivity was quantitatively less. The differences may result to some degree from the fact that the chemicals we chose have different mitochondrial mechanisms of toxicity, as well as different non-mitochondrial effects. Rotenone is an ETC CI inhibitor, DNP is a mitochondrial uncoupler, paraquat is a redox cycler, cisplatin can induce irreparable mtDNA damage (Podratz et al. 2011), AfB_1 is a genotoxin capable of inducing irreparable mtDNA damage (González-Hunt et al. 2014; Niranjan et al. 1982), while arsenite can induce ROS and inhibit enzymes (Kitchin and Wallace 2008; Shi et al. 2004; Zhao et al. 1997). Results are further complicated by the fact that many of the tested genes have additional roles beyond fission, fusion, and mitophagy. For example, *pink-1* can regulate ETC CI activity through phosphorylation (Morais et al. 2014), which may explain why *pink-1*-, but not *pdr-1*-deficient nematodes are hypersensitive to rotenone. A limitation to our chemical screen is that we limited the screen to larval growth; longer-term analyses could potentially uncover other sensitivities if, for example, effects of fission or mitophagy deficiency manifest over a longer time-course.

Overall, these results strongly support the importance of mitochondrial fusion in limiting mitochondrial toxicity. These results are consistent with emerging literature, as exposure to manganese, 6-hydroxydopamine, or glutamate induce mitochondrial fission and dysfunction; however, inhibiting fission prevents toxicity (Alaimo et al. 2014; Gomez-Lazaro et al. 2008; Grohm et al. 2012). One explanation for this is that mitochondrial fusion promotes functional complementation, which can limit the impact of toxicant-induced damage. In further support of this, we have previously reported hyper-fused mitochondrial networks in *drp-1*-, *pink-1-,* and *pdr-1*-deficient nematodes (Luz et al. 2015a); thus, it is conceivable that the hyper-fused phenotype provides buffering capacity against damage, helping to explain why more severe toxicant responses were not observed in fission- and mitophagy-deficient nematodes. We have previously noted similar patterns of strong sensitivity of fusion mutants, but mild sensitivity of fission and mitophagy mutants, in response to persistent mitochondrial DNA damage induced by ultraviolet light (Bess et al. 2012; Bess et al. 2013). Alternatively, mitophagy is a biologically slow process compared to fission, fusion, and functional complementation (Abeliovich et al. 2013; Geisler et al. 2010). Severely damaged mitochondria are initially prevented from rejoining the mitochondrial network through the proteasomal cleavage of OPA1 (*eat-3* homolog), thus preventing fusion prior to mitophagy (Head et al. 2009). The slower kinetics of mitophagy may explain why mitophagy-deficient nematodes did not display higher sensitivity to toxicants, as initial damage can be limited via more rapid stress response pathways. On the other hand, phosphorylation of MFN2 (*fzo-1*

homolog) by *pink-1* is required for the recruitment of parkin and subsequent mitophagy (Chen and Dorn 2013); thus, impaired mitophagy may also contribute to the sensitivity of *fzo-1*-deficient nematodes to some toxicants.

Unexpectedly, fission-, fusion-, and mitophagy-deficient nematodes displayed resistance to acrolein, a highly reactive air pollutant capable of inducing irreparable damage and mutations in mtDNA (Kasiviswanathan et al. 2013; Sun et al. 2006). However, resistance to acrolein has been observed in *D. melanogaster* strains with reduced metabolic rate, which is likely due to reduced toxicant uptake due to diminished oxygen consumption (Barros et al. 1991). As we and other have shown altered metabolism in fission, fusion, and mitophagy-deficient nematodes (Luz et al. 2015a; Palikaras et al. 2015), it is likely that similar mechanisms underlie acrolein resistance in nematodes. Resistance to cadmium, a metal capable of inhibiting mitochondrial function through protein thiol binding (Biagioli et al. 2008; Dorta et al. 2003; Rikans and Yamano 2000; Sokolova et al. 2005), was also observed in *fzo-1*. In addition to fusion, MFN2 (*fzo-1* homolog) also plays a role in tethering mitochondria to the endoplasmic reticulum (ER) allowing redox and calcium signaling to occur between the two organelles (Sugiura et al. 2013). As the ER is a major site of calcium storage, and is a target of cadmium toxicity due to molecular mimicry (Biagioli et al. 2008), it is possible that impaired ER-mitochondrial interactions due to a loss of *fzo-1* would reduce the inadvertent transfer of cadmium from the ER to the mitochondria resulting in the observed resistance.

4.2 Arsenite increases mitochondrial function in wild-type but not fusion-deficient nematodes

Arsenite increased mitochondrial function in 8-day old wild-type nematodes, causing an increase in basal OCR, maximal OCR, spare respiratory capacity (trending increase), citrate synthase and ETC CI activity. Both CS and ETC CI activity have been shown to correlate well with mitochondrial content (Larsen et al. 2012), which suggests an induction of mitochondrial biogenesis. Interestingly, arsenite can also induce mitochondrial biogenesis and enhance mitochondrial function in human keratinocytes through an upregulation of *TFAM* (Lee et al. 2011). However, under the conditions of our experiments, arsenite did not detectably alter expression of mitochondrial biogenesis genes (*polg-1, hmg-5*) or mtDNA-specific transcripts (*nd-5, ctb-1*), nor did arsenite induce mitochondrial fusion, a process also associated with increased metabolic activity (Pich et al. 2005; Westermann 2012), or increase expression of mitochondrial targeted GFP in body wall muscle cells. These conflicting results suggest increased mitochondrial function may not be due to increased biogenesis, but rather due to some other as-yet unidentified mechanism. For example, post-translation modifications (Hofer and Wenz 2014) or positive allosteric regulation (Das and Harris 1990; McCormack and Denton 1994) of OXPHOS may be playing a role; however, additional work is required to test this.

Emerging evidence suggests arsenite can induce hormesis at low doses. Evidence for arsenite-induced hormesis includes reduced risk of developing skin cancer in Denmark (Baastrup et al. 2008), increased growth advantage for cells in culture (Schmeisser et al. 2013; Snow et al. 2005), and lifespan extension, stress resistance, and increased

mitochondrial respiration in *C. elegans* (Schmeisser et al. 2013). However, we do not interpret the increase in mitochondrial function that we observed in wild-type nematodes as a classic hormetic response. First, the concentrations of arsenite used in the present study are high (100μM) compared to concentrations of arsenite previously found to induce hormesis in nematodes (100nM arsenite) (Schmeisser et al. 2013), and the exposure was to 8-day old nematodes, not larvae, the lifestage in which hormetic effects are most frequently tested in *C. elegans*. Second, increased stress resistance did not accompany the enhancement in mitochondrial function. Instead, arsenite exposure increased sensitivity to the redox stressor paraquat. Third, patients with arsenic-induced Bowen's disease (BD; cutaneous carcinoma) exhibit increased mitochondrial biogenesis compared to both healthy and non-arsenic-induced BD patients, and enhanced mitochondrial function provides a proliferative advantage for malignant cells (Lee et al. 2011). Thus, increased mitochondrial function in wild-type nematodes may represent an aberrant change in metabolism preceding pathogenesis. However, it is also possible that enhanced mitochondrial function is part of the nematode stress response. In support of this, nematodes can extrude arsenite via the ArsA ATPase (Tseng et al. 2007). Although stimulating pyruvate metabolism with DCA treatment did not reduce sensitivity to arsenite, it is unclear if ATP is rate limiting or if DCA treatment can overcome arsenite-induced PDH inhibition; thus, we cannot fully exclude this mechanism.

Importantly, the internal dose of arsenite measured in wild-type nematodes (69.5μg/L) is within the range (2.9 – 74.6μg/L) measured in blood samples taken from humans exposed to arsenic-contaminated drinking water (Hall et al. 2007; Valentine et al. 1979). The discrepancy between the high arsenite concentrations in the dosing media and internal concentrations is likely due to the nematode cuticle, a collagenous barrier that can limit uptake of certain compounds, including metals such as manganese (Au et al. 2009; Partridge et al. 2008).

Finally, irrespective of whether or not the term "hormesis" could be applied in our experiments with wild-type nematodes, it was striking that none of the potentially beneficial changes were observed in the fusion-deficient nematodes, which were sensitive to arsenite toxicity. This supports the idea that the process of mitochondrial fusion is a critical mechanism of mitochondrial stress resistance, an idea further supported by other findings in this study.

4.3 Deficiencies in mitochondrial fusion sensitize C. elegans to arsenite-induced mitochondrial dysfunction

Mitochondrial fission and fusion are dynamic processes that control mitochondrial morphology and stress response (Chan 2012). Interestingly, fusion-deficient nematodes were sensitive to arsenite in all toxicity assays (growth, lethality, mitochondrial dysfunction) and at all life stages (L1, L4, 8- and 12-days of age), while sensitivity appears to be life stage specific for *drp-1* nematodes, or may require more time to manifest. Furthermore, sensitivity to arsenite increased, relative to wild-type, as *drp-1* nematodes age. This is demonstrated by the fact that no sensitivity to arsenite was observed for *drp-1* in larval growth or L4 stage lethality assays (24h exposure), while sensitivity was observed in reproduction (48h L4

exposure), and lethality assays at 8 and 12 days of age. Furthermore, arsenite only induced mitochondrial dysfunction in 12-day old *drp-1* nematodes, despite the fact that 8-day old *drp-1* nematodes had higher intracellular arsenite concentrations compared to wild-type nematodes. The apparent age-dependent increase in sensitivity to arsenite may be explained by the fact that deficiencies in mitochondrial fission can result in impaired mitophagy and accumulation of damaged macromolecules (Bess et al. 2012; Twig et al. 2008). Thus, the natural buffering effect that accompanies hyperfusion in *drp-1* nematodes may be lost as nematodes accumulate damage throughout aging, and may help to explain the age-related increase in arsenite sensitivity.

Despite decades of research, the precise mechanisms underlying arsenic-induced disease remain poorly understood; however, generation of ROS (Shi et al. 2004), enzyme inhibition by sulfhydryl group binding (Kitchin and Wallace 2008), and alterations in DNA methylation (Zhao et al. 1997) are all believed to play a role. In agreement with previous reports (Liao and Yu 2005; Luz et al. 2016a; Sahu et al. 2013), arsenite induced the expression of superoxide dismutase and heat-shock protein genes, suggesting a role for ROS and protein misfolding in arsenite toxicity in nematodes. Interestingly, arsenite only induced mitochondrial-specific *hsp-6* expression in *fzo-1* and *eat-3* nematodes, which suggests a disruption of mitochondrial proteostasis. In agreement with this, arsenite inhibited both pyruvate (PDH) and isocitrate (IDH) dehydrogenase activity in *fzo-1*- and *eat-3*-deficient nematodes, suggesting a disruption of pyruvate metabolism and Krebs cycle activity. As the Krebs cycle is major source of the reducing equivalents NADH and $FADH_2$, which feed electrons into complex I and complex II of the ETC, respectively, disruption of the Krebs cycle may cause mitochondrial dysfunction in fusion-deficient nematodes through substrate limitation.

Collectively, our results and others' suggest that mitochondrial proteins are one of many targets of arsenite, but that deficiency in mitochondrial fusion sensitizes by elevating the relative importance of those targets by reducing the adaptive mitochondrial stress response. Previously we have shown that longer exposures to similar concentrations of arsenite (48h exposure to 50–500μM) disrupt pyruvate metabolism, induce severe mitochondrial dysfunction, and increase glycolysis in germline-deficient, but otherwise wild-type nematode strains (Luz et al. 2016a). Furthermore, mild mitochondrial dysfunction is observed in wild-type nematodes following longer (48h) arsenite exposures. This supports the idea that the mechanism by which arsenite induces mitochondrial dysfunction (i.e. disruption of pyruvate metabolism and Krebs cycle activity) in *fzo-1, eat-3,* wild-type, and germline-deficient nematodes is conserved, but that mitodynamic deficiency effectively lowers the dose-response. Furthermore, no evidence of a compensatory increase in glycolysis was observed in fusion-deficient nematodes. Fragmented mitochondrial networks *per se* do not appear to be the main driver of toxicity, as *fzo-1; drp-1* double mutants in which mitochondrial morphology is restored to a wild-type phenotype (Breckenridge et al. 2008) display similar sensitivity to arsenite as *fzo-1* nematodes. This suggests that it is the capacity for a dynamic response itself that permits an adaptive response. While additional work will be required to fully elucidate the mechanisms of this response, it is probable that a combination of factors, including impaired damage removal (Bess et al. 2012), a loss of functional complementation, and reduced metabolic plasticity (Luz et al. 2015a; Palikaras et

al. 2015), all contribute to arsenite sensitivity in fusion-deficient nematodes. Most importantly, these results collectively suggest that individuals carrying mutations in mitochondrial fusion genes (OPA1, MFN2) may be especially sensitive to arsenite toxicity, and warrant further investigation among people exposed to arsenic and other mitotoxicants.

Supplementary Material

Refer to Web version on PubMed Central for supplementary material.

Acknowledgments

This work was supported by the National Institutes of Environmental Health Sciences [R01-ES017540-01A2 and P42ES010356 to JNM, F31ES026859 to ALL].

Abbreviations

OMM	outer mitochondrial membrane
DRP1	dynamin-related protein-1
MFN1	mitofusin 1
MFN2	mitofusin 2
mtDNA	mitochondrial DNA
PINK1	PTEN-induced putative kinase 1
PARK2	parkin
DOA	dominant optic atrophy
CMT2A	Charcot-Marie-Tooth neuropathy type 2A
PD	Parkinson’s Disease
DNP	2,4-dinitrophenol
AfB_1	aflatoxin B_1
L1	larval stage 1
ToF	Time of flight
nucDNA	nuclear DNA
PDH	pyruvate dehydrogenase
IDH	isocitrate dehydrogenase
ROS	reactive oxygen species
UPR	unfolded protein response
OXPHOS	oxidative phosphorylation

OCR	oxygen consumption rate
SRC	spare respiratory capacity
3-MA	3-methyladenine
HSP	heat-shock protein
2-DG	2-deoxy-D-glucose
DCA	dichloroacetate
CS	citrate synthase

References

Abeliovich H, Zarei M, Rigbolt KT, Youle RJ, Dengjel J. Involvement of mitochondrial dynamics in the segregation of mitochondrial matrix proteins during stationary phase mitophagy. Nature communications. 2013; 4

Ahn JM, Eom HJ, Yang X, Meyer JN, Choi J. Comparative toxicity of silver nanoparticles on oxidative stress and DNA damage in the nematode, Caenorhabditis elegans. Chemosphere. 2014; 108:343–352. [PubMed: 24726479]

Alaimo A, Gorojod RM, Beauquis J, Munoz MJ, Saravia F, Kotler ML. Deregulation of mitochondria-shaping proteins Opa-1 and Drp-1 in manganese-induced apoptosis. PLoS One. 2014; 9:e91848. [PubMed: 24632637]

Anderson GL, Boyd WA, Williams P. Assessment of sublethal endpoints for toxicity testing with the nematode Caenorhabditis elegans. Environmental Toxicology and Chemistry. 2001; 20:833–838. [PubMed: 11345460]

Au C, Benedetto A, Anderson J, Labrousse A, Erikson K, Ewbank JJ, Aschner M. SMF-1, SMF-2 and SMF-3 DMT1 orthologues regulate and are regulated differentially by manganese levels in C. elegans. PloS one. 2009; 4:e7792. [PubMed: 19924247]

Baastrup R, Sørensen M, Balstrøm T, Frederiksen K, Larsen CL, Tjønneland A, Overvad K, Raaschou-Nielsen O. Arsenic in drinking-water and risk for cancer in Denmark. Environmental Health Perspectives. 2008; 116:231. [PubMed: 18288323]

Bailey DC, Todt CE, Orfield SE, Denney RD, Snapp IB, Negga R, Montgomery KM, Bailey AC, Pressley AS, Traynor WL. Caenorhabditis elegans chronically exposed to a Mn/Zn ethylene-bis-dithiocarbamate fungicide show mitochondrial Complex I inhibition and increased reactive oxygen species. NeuroToxicology. 2016; 56:170–179. [PubMed: 27502893]

Barros A, Sierra L, Comendador M. Decreased metabolic rate as an acrolein resistance mechanism inDrosophila melanogaster. Behavior genetics. 1991; 21:445–451. [PubMed: 1776945]

Bergquist ER, Fischer RJ, Sugden KD, Martin BD. Inhibition by methylated organoarsenicals of the respiratory 2-oxo-acid dehydrogenases. Journal of organometallic chemistry. 2009; 694:973–980. [PubMed: 20161290]

Bess AS, Crocker TL, Ryde IT, Meyer JN. Mitochondrial dynamics and autophagy aid in removal of persistent mitochondrial DNA damage in Caenorhabditis elegans. Nucleic acids research. 2012; 40:7916–7931. [PubMed: 22718972]

Bess AS, Leung MC, Ryde IT, Rooney JP, Hinton DE, Meyer JN. Effects of mutations in mitochondrial dynamics-related genes on the mitochondrial response to ultraviolet C radiation in developing Caenorhabditis elegans. Worm, Taylor & Francis. 2013:e23763.

Biagioli M, Pifferi S, Ragghianti M, Bucci S, Rizzuto R, Pinton P. Endoplasmic reticulum stress and alteration in calcium homeostasis are involved in cadmium-induced apoptosis. Cell calcium. 2008; 43:184–195. [PubMed: 17588656]

Bolt AM, Douglas RM, Klimecki WT. Arsenite exposure in human lymphoblastoid cell lines induces autophagy and coordinated induction of lysosomal genes. Toxicology letters. 2010; 199:153–159. [PubMed: 20816728]

Bonifati V, Rohe C, Breedveld G, Fabrizio E, De Mari M, Tassorelli C, Tavella A, Marconi R, Nicholl D, Chien H. Early-onset parkinsonism associated with PINK1 mutations Frequency, genotypes, and phenotypes. Neurology. 2005; 65:87–95. [PubMed: 16009891]

Boyd WA, Smith MV, Kissling GE, Freedman JH. Medium-and high-throughput screening of neurotoxicants using C. elegans. Neurotoxicology and teratology. 2010; 32:68–73. [PubMed: 19166924]

Breckenridge DG, Kang BH, Kokel D, Mitani S, Staehelin LA, Xue D. Caenorhabditis elegans drp-1 and fis-2 regulate distinct cell-death execution pathways downstream of ced-3 and independent of ced-9. Molecular cell. 2008; 31:586–597. [PubMed: 18722182]

Brys K, Vanfleteren JR, Braeckman BP. Testing the rate-of-living/oxidative damage theory of aging in the nematode model Caenorhabditis elegans. Exp Gerontol. 2007; 42:845–851. [PubMed: 17379464]

Cartoni R, Martinou JC. Role of mitofusin 2 mutations in the physiopathology of Charcot–Marie–Tooth disease type 2A. Experimental neurology. 2009; 218:268–273. [PubMed: 19427854]

Cassidy-Stone A, Chipuk JE, Ingerman E, Song C, Yoo C, Kuwana T, Kurth MJ, Shaw JT, Hinshaw JE, Green DR. Chemical inhibition of the mitochondrial division dynamin reveals its role in Bax/Bak-dependent mitochondrial outer membrane permeabilization. Developmental cell. 2008; 14:193–204. [PubMed: 18267088]

Chan DC. Mitochondrial fusion and fission in mammals. Annu Rev Cell Dev Biol. 2006; 22:79–99. [PubMed: 16704336]

Chan DC. Fusion and fission: interlinked processes critical for mitochondrial health. Annual review of genetics. 2012; 46:265–287.

Chen Y, Dorn GW. PINK1-phosphorylated mitofusin 2 is a Parkin receptor for culling damaged mitochondria. Science. 2013; 340:471–475. [PubMed: 23620051]

Choi BO, Nakhro K, Park H, Hyun Y, Lee J, Kanwal S, Jung SC, Chung K. A cohort study of MFN2 mutations and phenotypic spectrums in Charcot–Marie–Tooth disease 2A patients. Clinical genetics. 2015; 87:594–598. [PubMed: 24863639]

Chowdhury M, Uddin M, Ahmed M, Ali M, Uddin S. How does arsenic contamination of groundwater causes severity and health hazard in Bangladesh. Journal of Applied Sciences. 2006; 6:1275–1286.

Croteau DL, DellaVecchia MJ, Perera L, Van Houten B. Cooperative damage recognition by UvrA and UvrB: identification of UvrA residues that mediate DNA binding. DNA repair. 2008; 7:392–404. [PubMed: 18248777]

Das AM, Harris DA. Control of mitochondrial ATP synthase in heart cells: inactive to active transitions caused by beating or positive inotropic agents. Cardiovascular research. 1990; 24:411–417. [PubMed: 1695547]

Delettre C, Lenaers G, Griffoin JM, Gigarel N, Lorenzo C, Belenguer P, Pelloquin L, Grosgeorge J, Turc-Carel C, Perret E. Nuclear gene OPA1, encoding a mitochondrial dynamin-related protein, is mutated in dominant optic atrophy. Nature genetics. 2000; 26:207–210. [PubMed: 11017079]

Ditzel EJ, Nguyen T, Parker P, Camenisch TD. Effects of Arsenite Exposure during Fetal Development on Energy Metabolism and Susceptibility to Diet-Induced Fatty Liver Disease in Male Mice. Environmental health perspectives. 2015; 124:201–209. [PubMed: 26151952]

Dorta DJ, Leite S, DeMarco KC, Prado IM, Rodrigues T, Mingatto FE, Uyemura SA, Santos AC, Curti C. A proposed sequence of events for cadmium-induced mitochondrial impairment. Journal of inorganic biochemistry. 2003; 97:251–257. [PubMed: 14511887]

Elachouri G, Vidoni S, Zanna C, Pattyn A, Boukhaddaoui H, Gaget K, Yu-Wai-Man P, Gasparre G, Sarzi E, Delettre C. OPA1 links human mitochondrial genome maintenance to mtDNA replication and distribution. Genome research. 2011; 21:12–20. [PubMed: 20974897]

Estornell E, Fato R, Pallotti F, Lenaz G. Assay conditions for the mitochondrial NADH: coenzyme Q oxidoreductase. FEBS letters. 1993; 332:127–131. [PubMed: 8405427]

Feely S, Laura M, Siskind C, Sottile S, Davis M, Gibbons V, Reilly M, Shy M. MFN2 mutations cause severe phenotypes in most patients with CMT2A. Neurology. 2011; 76:1690–1696. [PubMed: 21508331]

Geisler S, Holmström KM, Skujat D, Fiesel FC, Rothfuss OC, Kahle PJ, Springer W. PINK1/Parkin-mediated mitophagy is dependent on VDAC1 and p62/SQSTM1. Nature cell biology. 2010; 12:119–131. [PubMed: 20098416]

Gilbert-Diamond D, Li Z, Perry AE, Spencer SK, Gandolfi AJ, Karagas MR. A population-based case–control study of urinary arsenic species and squamous cell carcinoma in New Hampshire, USA. Environmental health perspectives. 2013; 121:1154. [PubMed: 23872349]

Gomez-Lazaro M, Bonekamp NA, Galindo MF, Jordan J, Schrader M. 6-Hydroxydopamine (6-OHDA) induces Drp1-dependent mitochondrial fragmentation in SH-SY5Y cells. Free radical biology & medicine. 2008; 44:1960–1969. [PubMed: 18395527]

González-Hunt CP, Leung MC, Bodhicharla RK, McKeever MG, Arrant AE, Margillo KM, Ryde IT, Cyr DD, Kosmaczewski SG, Hammarlund M. Exposure to mitochondrial genotoxins and dopaminergic neurodegeneration in Caenorhabditis elegans. PloS one. 2014; 9:e114459. [PubMed: 25486066]

Gonzalez-Hunt CP, Rooney JP, Ryde IT, Anbalagan C, Joglekar R, Meyer JN. PCR-Based Analysis of Mitochondrial DNA Copy Number, Mitochondrial DNA Damage, and Nuclear DNA Damage. Current Protocols in Toxicology. 2016:20.11.21–20.11.25.

Grohm J, Kim SW, Mamrak U, Tobaben S, Cassidy-Stone A, Nunnari J, Plesnila N, Culmsee C. Inhibition of Drp1 provides neuroprotection in vitro and in vivo. Cell death and differentiation. 2012; 19:1446–1458. [PubMed: 22388349]

Hall M, Gamble M, Slavkovich V, Liu X, Levy D, Cheng Z, Van Geen A, Yunus M, Rahman M, Pilsner JR. Determinants of arsenic metabolism: blood arsenic metabolites, plasma folate, cobalamin, and homocysteine concentrations in maternal-newborn pairs. Environmental health perspectives. 2007:1503–1509. [PubMed: 17938743]

Head B, Griparic L, Amiri M, Gandre-Babbe S, van der Bliek AM. Inducible proteolytic inactivation of OPA1 mediated by the OMA1 protease in mammalian cells. The Journal of cell biology. 2009; 187:959–966. [PubMed: 20038677]

Higashi T, Maruyama E, Otani T, Sakamoto Y. Studies on the Isocitrate Dehydrogenase. The Journal of Biochemistry. 1965; 57:793–798. [PubMed: 4378751]

Hofer A, Wenz T. Post-translational modification of mitochondria as a novel mode of regulation. Experimental gerontology. 2014; 56:202–220. [PubMed: 24632076]

Hoogewijs D, Houthoofd K, Matthijssens F, Vandesompele J, Vanfleteren JR. Selection and validation of a set of reliable reference genes for quantitative sod gene expression analysis in C. elegans. BMC molecular biology. 2008; 9:1. [PubMed: 18177499]

Hosseini MJ, Shaki FS, Ghazi-Khansari M, Pourahmad J. Toxicity of arsenic (III) on isolated liver mitochondria: a new mechanistic approach. Iranian Journal of Pharmaceutical Research. 2013; 12:121–138. [PubMed: 24250680]

Johnson D, Nehrke K. Mitochondrial fragmentation leads to intracellular acidification in Caenorhabditis elegans and mammalian cells. Molecular biology of the cell. 2010; 21:2191–2201. [PubMed: 20444981]

Kanazawa T, Zappaterra MD, Hasegawa A, Wright AP, Newman-Smith ED, Buttle KF, McDonald K, Mannella CA, van der Bliek AM. The C. elegans Opa1 homologue EAT-3 is essential for resistance to free radicals. PLoS Genet. 2008; 4:e1000022. [PubMed: 18454199]

Karagas MR, Tosteson TD, Morris JS, Demidenko E, Mott LA, Heaney J, Schned A. Incidence of transitional cell carcinoma of the bladder and arsenic exposure in New Hampshire. Cancer Causes & Control. 2004; 15:465–472. [PubMed: 15286466]

Kasiviswanathan R, Minko IG, Lloyd RS, Copeland WC. Translesion synthesis past acrolein-derived DNA adducts by human mitochondrial DNA polymerase γ. Journal of Biological Chemistry. 2013; 288:14247–14255. [PubMed: 23543747]

Kim I, Lemasters JJ. Mitophagy selectively degrades individual damaged mitochondria after photoirradiation. Antioxidants & redox signaling. 2011; 14:1919–1928. [PubMed: 21126216]

Kitchin KT, Wallace K. The role of protein binding of trivalent arsenicals in arsenic carcinogenesis and toxicity. Journal of inorganic biochemistry. 2008; 102:532–539. [PubMed: 18164070]

Klein C, Westenberger A. Genetics of Parkinson's disease. Cold Spring Harbor perspectives in medicine. 2012; 2:a008888. [PubMed: 22315721]

Larsen S, Nielsen J, Hansen CN, Nielsen LB, Wibrand F, Stride N, Schroder HD, Boushel R, Helge JW, Dela F. Biomarkers of mitochondrial content in skeletal muscle of healthy young human subjects. The Journal of physiology. 2012; 590:3349–3360. [PubMed: 22586215]

Lee CH, Wu SB, Hong CH, Liao WT, Wu CY, Chen GS, Wei YH, Yu HS. Aberrant cell proliferation by enhanced mitochondrial biogenesis via mtTFA in arsenical skin cancers. The American journal of pathology. 2011; 178:2066–2076. [PubMed: 21514422]

Lewis JA, Fleming JT. Basic culture methods. Methods in cell biology. 1995; 48:3–29. [PubMed: 8531730]

Li R, Kou X, Geng H, Xie J, Yang Z, Zhang Y, Cai Z, Dong C. Effect of ambient PM(2.5) on lung mitochondrial damage and fusion/fission gene expression in rats. Chem Res Toxicol. 2015; 28:408–418. [PubMed: 25560372]

Liao VHC, Yu CW. Caenorhabditis elegans gcs-1 confers resistance to arsenic-induced oxidative stress. Biometals. 2005; 18:519–528. [PubMed: 16333752]

Luz AL, Godebo TR, Bhatt DP, Ilkayeva OR, Maurer LL, Hirschey MD, Meyer JN. Arsenite uncouples mitochondrial respiration and induces a Warburg-like effect in Caenorhabditis elegans. Toxicological sciences: an official journal of the Society of Toxicology. 2016a

Luz AL, Lagido C, Hirschey MD, Meyer JN. In Vivo Determination of Mitochondrial Function Using Luciferase-Expressing Caenorhabditis elegans: Contribution of Oxidative Phosphorylation, Glycolysis, and Fatty Acid Oxidation to Toxicant-Induced Dysfunction. Current Protocols in Toxicology. 2016b:25.28.21–25.28.22. [PubMed: 27479364]

Luz AL, Rooney JP, Kubik LL, Gonzalez CP, Song DH, Meyer JN. Mitochondrial morphology and fundamental parameters of the mitochondrial respiratory chain are altered in Caenorhabditis elegans strains deficient in mitochondrial dynamics and homeostasis processes. PloS one. 2015a; 10:e0130940. [PubMed: 26106885]

Luz AL, Smith LL, Rooney JP, Meyer JN. Seahorse Xfe24 Extracellular Flux Analyzer-Based Analysis of Cellular Respiration in Caenorhabditis elegans. Current Protocols in Toxicology. 2015b:25.27.21–25.27.15.

Lv H, Wang L, Zhang W, Wang Z, Zuo Y, Liu J, Yuan Y. A cohort study of Han Chinese MFN2-related Charcot–Marie–Tooth 2A. Journal of the neurological sciences. 2015; 358:153–157. [PubMed: 26382835]

Maglioni S, Ventura N. C. elegans as a model organism for human mitochondrial associated disorders. Mitochondrion. 2016

Marshall G, Ferreccio C, Yuan Y, Bates MN, Steinmaus C, Selvin S, Liaw J, Smith AH. Fifty-year study of lung and bladder cancer mortality in Chile related to arsenic in drinking water. Journal of the National Cancer Institute. 2007; 99:920–928. [PubMed: 17565158]

McBride HM, Neuspiel M, Wasiak S. Mitochondria: more than just a powerhouse. Current Biology. 2006; 16:R551–R560. [PubMed: 16860735]

McCormack J, Denton R. Mitochondrial Ca2+ transport and the role of intramitochondrial Ca2+ in the regulation of energy metabolism. Developmental neuroscience. 1994; 15:165–173.

Meyer JN, Boyd WA, Azzam GA, Haugen AC, Freedman JH, Van Houten B. Decline of nucleotide excision repair capacity in aging Caenorhabditis elegans. Genome Biol. 2007; 8:R70. [PubMed: 17472752]

Morais VA, Haddad D, Craessaerts K, De Bock PJ, Swerts J, Vilain S, Aerts L, Overbergh L, Grünewald A, Seibler P. PINK1 loss-of-function mutations affect mitochondrial complex I activity via NdufA10 ubiquinone uncoupling. Science. 2014; 344:203–207. [PubMed: 24652937]

Murfitt RR, Vogel K, Sanadi DR. Characterization of the mitochondria of the free-living nematode, Caenorhabditis elegans. Comparative biochemistry and physiology. B, Comparative biochemistry. 1976; 53:423–430. [PubMed: 131020]

Nakada K, Inoue K, Ono T, Isobe K, Ogura A, Goto Y-i, Nonaka I, Hayashi JI. Inter-mitochondrial complementation: mitochondria-specific system preventing mice from expression of disease phenotypes by mutant mtDNA. Nature medicine. 2001; 7:934–940.

Ng LF, Gruber J, Cheah IK, Goo CK, Cheong WF, Shui G, Sit KP, Wenk MR, Halliwell B. The mitochondria-targeted antioxidant MitoQ extends lifespan and improves healthspan of a transgenic

Caenorhabditis elegans model of Alzheimer disease. Free Radical Biology and Medicine. 2014; 71:390–401. [PubMed: 24637264]

Niranjan B, Bhat N, Avadhani N. Preferential attack of mitochondrial DNA by aflatoxin B1 during hepatocarcinogenesis. Science. 1982; 215:73–75. [PubMed: 6797067]

Nuytemans K, Theuns J, Cruts M, Van Broeckhoven C. Genetic etiology of Parkinson disease associated with mutations in the SNCA, PARK2, PINK1, PARK7, and LRRK2 genes: a mutation update. Human mutation. 2010; 31:763–780. [PubMed: 20506312]

O'Riordan VB, Burnell AM. Intermediary metabolism in the dauer larva of the nematode Caenorhabditis elegans—1. Glycolysis, gluconeogenesis, oxidative phosphorylation and the tricarboxylic acid cycle. Comparative Biochemistry and Physiology Part B: Comparative Biochemistry. 1989; 92:233–238.

Okimoto R, Macfarlane JL, Clary DO, Wolstenholme DR. The mitochondrial genomes of two nematodes, Caenorhabditis elegans and Ascaris suum. Genetics. 1992; 130:471–498. [PubMed: 1551572]

Palikaras K, Lionaki E, Tavernarakis N. Coordination of mitophagy and mitochondrial biogenesis during ageing in C. elegans. Nature. 2015; 521:525–528. [PubMed: 25896323]

Partridge FA, Tearle AW, Gravato-Nobre MJ, Schafer WR, Hodgkin J. The C. elegans glycosyltransferase BUS-8 has two distinct and essential roles in epidermal morphogenesis. Developmental biology. 2008; 317:549–559. [PubMed: 18395708]

Pich S, Bach D, Briones P, Liesa M, Camps M, Testar X, Palacín M, Zorzano A. The Charcot–Marie–Tooth type 2A gene product, Mfn2, up-regulates fuel oxidation through expression of OXPHOS system. Human molecular genetics. 2005; 14:1405–1415. [PubMed: 15829499]

Podratz JL, Knight AM, Ta LE, Staff NP, Gass JM, Genelin K, Schlattau A, Lathroum L, Windebank AJ. Cisplatin induced mitochondrial DNA damage in dorsal root ganglion neurons. Neurobiology of disease. 2011; 41:661–668. [PubMed: 21145397]

Rambold AS, Kostelecky B, Elia N, Lippincott-Schwartz J. Tubular network formation protects mitochondria from autophagosomal degradation during nutrient starvation. Proceedings of the National Academy of Sciences. 2011; 108:10190–10195.

Ravenscroft, P., Brammer, H., Richards, K. Arsenic pollution: a global synthesis. John Wiley & Sons; 2009.

Rea SL, Ventura N, Johnson TE. Relationship between mitochondrial electron transport chain dysfunction, development, and life extension in Caenorhabditis elegans. PLoS Biol. 2007; 5:e259. [PubMed: 17914900]

Rikans LE, Yamano T. Mechanisms of cadmium-mediated acute hepatotoxicity. Journal of biochemical and molecular toxicology. 2000; 14:110–117. [PubMed: 10630425]

Rooney JP, Ryde IT, Sanders LH, Howlett EH, Colton MD, Germ KE, Mayer GD, Greenamyre JT, Meyer JN. PCR based determination of mitochondrial DNA copy number in multiple species. Mitochondrial Regulation: Methods and Protocols. 2015:23–38.

Sahu SN, Lewis J, Patel I, Bozdag S, Lee JH, Sprando R, Cinar HN. Genomic analysis of stress response against arsenic in Caenorhabditis elegans. PloS one. 2013; 8:e66431. [PubMed: 23894281]

Sanchez-Soria P, Broka D, Quach S, Hardwick RN, Cherrington NJ, Camenisch TD. Fetal exposure to arsenic results in hyperglycemia, hypercholesterolemia, and nonalcoholic fatty liver disease in adult mice. Journal of Toxicology and Health. 2014; 1:1.

Schaffer S, Gruber J, Ng L, Fong S, Wong Y, Tang S, Halliwell B. The effect of dichloroacetate on health-and lifespan in C. elegans. Biogerontology. 2011; 12:195–209. [PubMed: 21153705]

Schmeisser S, Schmeisser K, Weimer S, Groth M, Priebe S, Fazius E, Kuhlow D, Pick D, Einax JW, Guthke R. Mitochondrial hormesis links low-dose arsenite exposure to lifespan extension. Aging cell. 2013; 12:508–517. [PubMed: 23534459]

Schon EA, Gilkerson RW. Functional complementation of mitochondrial DNAs: mobilizing mitochondrial genetics against dysfunction. Biochimica et Biophysica Acta (BBA)-General Subjects. 2010; 1800:245–249. [PubMed: 19616602]

Shi H, Shi X, Liu KJ. Oxidative mechanism of arsenic toxicity and carcinogenesis. Molecular and cellular biochemistry. 2004; 255:67–78. [PubMed: 14971647]

Shi X, Wei X, Koo I, Schmidt RH, Yin X, Kim SH, Vaughn A, McClain CJ, Arteel GE, Zhang X. Metabolomic analysis of the effects of chronic arsenic exposure in a mouse model of diet-induced fatty liver disease. Journal of proteome research. 2013; 13:547–554. [PubMed: 24328084]

Snow ET, Sykora P, Durham TR, Klein CB. Arsenic, mode of action at biologically plausible low doses: what are the implications for low dose cancer risk? Toxicology and applied pharmacology. 2005; 207:557–564. [PubMed: 15996700]

Sokolova IM, Sokolov EP, Ponnappa KM. Cadmium exposure affects mitochondrial bioenergetics and gene expression of key mitochondrial proteins in the eastern oyster Crassostrea virginica Gmelin (Bivalvia: Ostreidae). Aquatic Toxicology. 2005; 73:242–255. [PubMed: 15935864]

Srere P. Citrate synthase:[EC 4.1. 3.7. Citrate oxaloacetate-lyase (CoA-acetylating)]. Methods in enzymology. 1969; 13:3–11.

Stiernagle T. Maintenance of C.elegans. C.elegans. 1999; 2:51–67.

Sugiura A, Nagashima S, Tokuyama T, Amo T, Matsuki Y, Ishido S, Kudo Y, McBride HM, Fukuda T, Matsushita N. MITOL regulates endoplasmic reticulum-mitochondria contacts via Mitofusin2. Molecular cell. 2013; 51:20–34. [PubMed: 23727017]

Sumitani M, Kasashima K, Matsugi J, Endo H. Biochemical properties of Caenorhabditis elegans HMG-5, a regulator of mitochondrial DNA. Journal of biochemistry. 2011; 149:581–589. [PubMed: 21258070]

Sun L, Luo C, Long J, Wei D, Liu J. Acrolein is a mitochondrial toxin: effects on respiratory function and enzyme activities in isolated rat liver mitochondria. Mitochondrion. 2006; 6:136–142. [PubMed: 16725382]

Thiselton DL, Alexander C, Morris A, Brooks S, Rosenberg T, Eiberg H, Kjer B, Kjer P, Bhattacharya SS, Votruba M. A frameshift mutation in exoná28 of the OPA1 gene explains the high prevalence of dominant optic atrophy in the Danish population: evidence for a founder effect. Human genetics. 2001; 109:498–502. [PubMed: 11735024]

Trounce IA, Kim YL, Jun AS, Wallace DC. Assessment of mitochondrial oxidative phosphorylation in patient muscle biopsies, lymphoblasts, and transmitochondrial cell lines. Methods in enzymology. 1996; 264:484–509. [PubMed: 8965721]

Tsang WY, Lemire BD. Mitochondrial genome content is regulated during nematode development. Biochemical and biophysical research communications. 2002; 291:8–16. [PubMed: 11829454]

Tsang WY, Lemire BD. The role of mitochondria in the life of the nematode, Caenorhabditis elegans. Biochimica et biophysica acta. 2003; 1638:91–105. [PubMed: 12853115]

Tsang WY, Sayles LC, Grad LI, Pilgrim DB, Lemire BD. Mitochondrial Respiratory Chain Deficiency inCaenorhabditis elegans Results in Developmental Arrest and Increased Life Span. Journal of Biological Chemistry. 2001; 276:32240–32246. [PubMed: 11410594]

Tseng YY, Yu CW, Liao VHC. Caenorhabditis elegans expresses a functional ArsA. FEBS Journal. 2007; 274:2566–2572. [PubMed: 17419726]

Twig G, Elorza A, Molina AJ, Mohamed H, Wikstrom JD, Walzer G, Stiles L, Haigh SE, Katz S, Las G. Fission and selective fusion govern mitochondrial segregation and elimination by autophagy. The EMBO journal. 2008; 27:433–446. [PubMed: 18200046]

Valentine JL, Kang HK, Spivey G. Arsenic levels in human blood, urine, and hair in response to exposure via drinking water. Environmental Research. 1979; 20:24–32. [PubMed: 499171]

Vanstone JR, Smith AM, McBride S, Naas T, Holcik M, Antoun G, Harper M-E, Michaud J, Sell E, Chakraborty P. DNM1L-related mitochondrial fission defect presenting as refractory epilepsy. European Journal of Human Genetics. 2015

Vinish M, Prabhakar S, Khullar M, Verma I, Anand A. Genetic screening reveals high frequency of PARK2 mutations and reduced Parkin expression conferring risk for Parkinsonism in North West India. Journal of Neurology, Neurosurgery & Psychiatry. 2010; 81:166–170.

Waterham HR, Koster J, van Roermund CW, Mooyer PA, Wanders RJ, Leonard JV. A lethal defect of mitochondrial and peroxisomal fission. New England Journal of Medicine. 2007; 356:1736–1741. [PubMed: 17460227]

Weber, CI. Methods for measuring the acute toxicity of effluents and receiving waters to freshwater and marine organisms. Environmental Monitoring Systems Laboratory, Office of Research and Development, US Environmental Protection Agency; 1991.

Westermann B. Bioenergetic role of mitochondrial fusion and fission. Biochimica et Biophysica Acta (BBA)-Bioenergetics. 2012; 1817:1833–1838. [PubMed: 22409868]

Whelan RS, Konstantinidis K, Wei AC, Chen Y, Reyna DE, Jha S, Yang Y, Calvert JW, Lindsten T, Thompson CB. Bax regulates primary necrosis through mitochondrial dynamics. Proceedings of the National Academy of Sciences. 2012; 109:6566–6571.

Youle RJ, Van Der Bliek AM. Mitochondrial fission, fusion, and stress. Science. 2012; 337:1062–1065. [PubMed: 22936770]

Yu-Wai-Man P, Griffiths PG, Burke A, Sellar PW, Clarke MP, Gnanaraj L, Ah-Kine D, Hudson G, Czermin B, Taylor RW. The prevalence and natural history of dominant optic atrophy due to OPA1 mutations. Ophthalmology. 2010; 117:1538–1546. e1531. [PubMed: 20417570]

Yu HS, Liao WT, Chai CY. Arsenic carcinogenesis in the skin. Journal of biomedical science. 2006; 13:657–666. [PubMed: 16807664]

Zhang T, Qi Y, Liao M, Xu M, Bower K, Frank J, Shen H-M, Luo J, Shi X, Chen G. Autophagy is a cell self-protective mechanism against arsenic-induced cell transfomation. Toxicological Sciences. 2012:kfs240.

Zhang Y, Zou X, Ding Y, Wang H, Wu X, Liang B. Comparative genomics and functional study of lipid metabolic genes in Caenorhabditis elegans. BMC genomics. 2013; 14:1. [PubMed: 23323973]

Zhao CQ, Young MR, Diwan BA, Coogan TP, Waalkes MP. Association of arsenic-induced malignant transformation with DNA hypomethylation and aberrant gene expression. Proceedings of the National Academy of Sciences. 1997; 94:10907–10912.

Zhao F, Severson P, Pacheco S, Futscher BW, Klimecki WT. Arsenic exposure induces the Warburg effect in cultured human cells. Toxicology and applied pharmacology. 2013; 271:72–77. [PubMed: 23648393]

Züchner S, Mersiyanova IV, Muglia M, Bissar-Tadmouri N, Rochelle J, Dadali EL, Zappia M, Nelis E, Patitucci A, Senderek J. Mutations in the mitochondrial GTPase mitofusin 2 cause Charcot-Marie-Tooth neuropathy type 2A. Nature genetics. 2004; 36:449–451. [PubMed: 15064763]

Zuryn S, Kuang J, Tuck A, Ebert PR. Mitochondrial dysfunction in Caenorhabditis elegans causes metabolic restructuring, but this is not linked to longevity. Mechanisms of ageing and development. 2010; 131:554–561. [PubMed: 20688098]

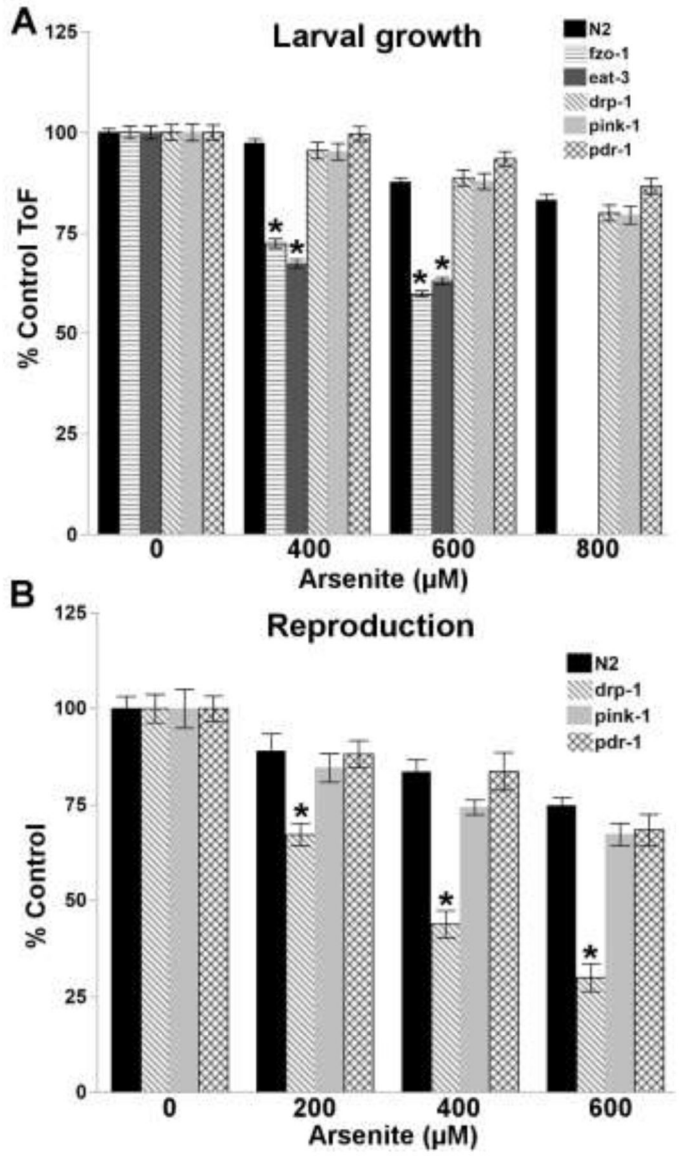

Fig. 1. Mitochondrial fusion- and fission-deficient nematodes are sensitive to arsenite

(A) *fzo-1*- and *eat-3*-deficient *C. elegans* are more sensitive to arsenite than wild-type (N2) nematodes in a 48h larval growth assay (two way ANOVA, arsenite, strain, interaction ($p<0.0001$ for all), N=471–1435). Larval growth was not measured for *fzo-1* or *eat-3* in the 800μM arsenite exposure group as significant lethality was observed. (B) *drp-1*-deficient nematodes were more susceptible to arsenite-induced reproductive toxicity than wild-type nematodes (two way ANOVA, arsenite, strain, interaction ($p<0.0001$ for all), N=11–19). Asterisk denotes statistical significance ($p<0.05$) for post-hoc comparison (Tukey's HSD) to N2 within each arsenite concentration. Bars ± SEM.

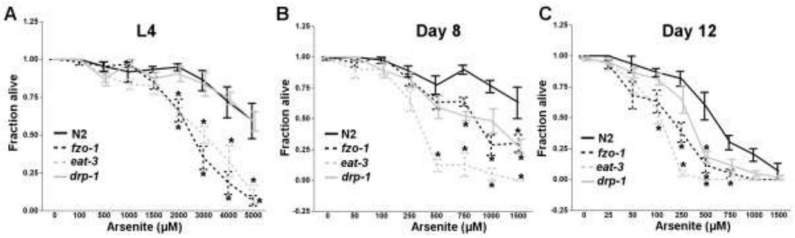

Figure 2. Deficiencies in *fzo-1*, *eat-3* and *drp-1* sensitize nematodes to arsenite-induced lethality throughout aging

Note different x-axes in different panels. (A) L4 stage, (B) 8-, and (C) 12-day old *fzo-1*- and *eat-3*-deficient nematodes are hypersensitive to arsenite-induced lethality compared to wild-type nematodes, while only (B) 8-, and (C) 12-day old *drp-1*-deficient nematodes display sensitivity (2 way ANOVA (at each lifestage), main effects of strain, arsenite and interaction ($p<0.0001$ for all)). Asterisk denotes statistical significance ($p<0.05$) for post-hoc comparison (Tukey's HSD) to N2 within each arsenite concentration. N=6–12. Bars±SEM.

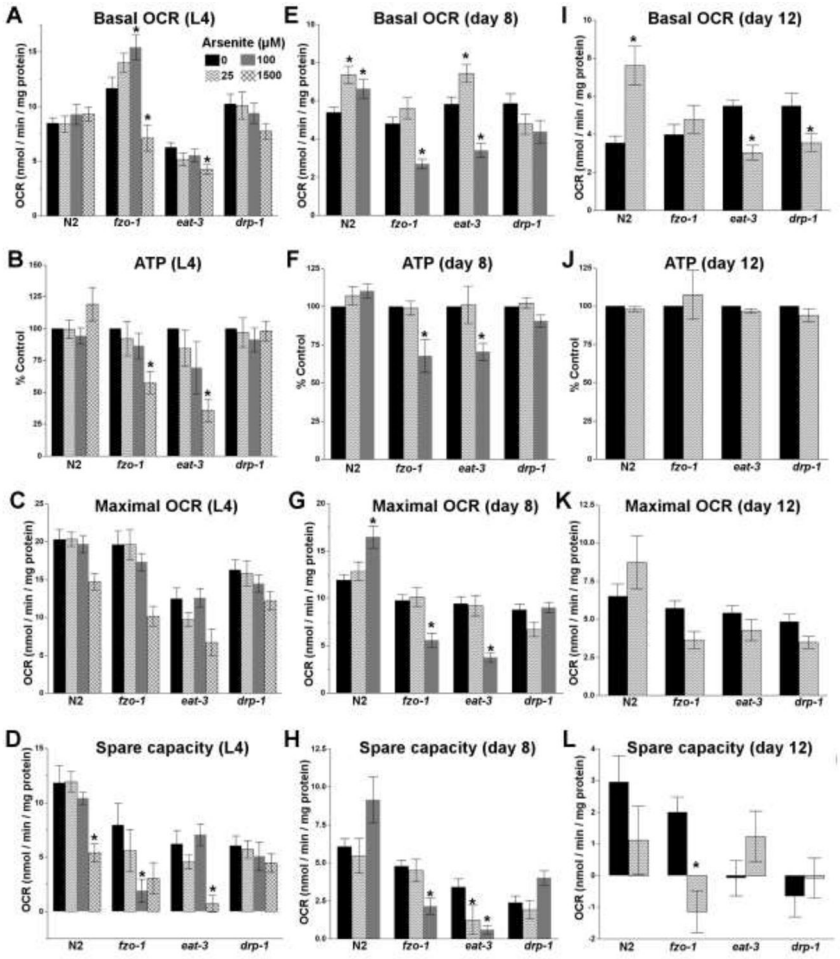

Figure 3. Arsenite disrupts mitochondrial function in fusion-deficient nematodes

Nematodes were exposure for 24h to non-lethal concentrations of arsenite, and then mitochondrial function (basal OCR, steady-state ATP, maximal OCR, and spare respiratory capacity) was assessed in (A–D) L4 stage, (E–H) 8-day old, and (I–L) 12-day old nematodes. P-values for statistical analysis are provided in Table S3. Asterisk denotes statistical significance ($p<0.05$) for post-hoc comparison (Tukey's HSD) to untreated control within each strain. N=11–13. Bars±SEM.

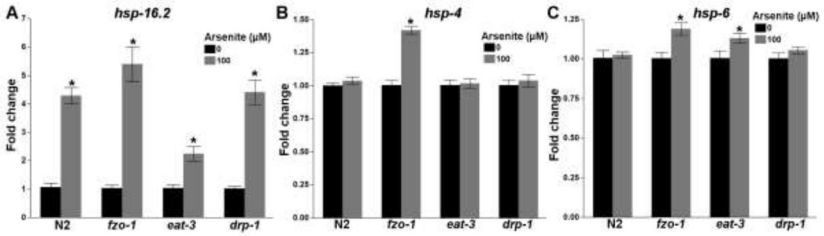

Figure 4. Arsenite induces the unfolded protein response

24h Exposure to 100μM arsenite in 8-day old nematodes induced (A) cytosolic *hsp-16.2* in all strains, (B) endoplasmic reticulum-specific *hsp-4* in *fzo-1*, and (C) mitochondrial-specific *hsp-6* in *fzo-1* and *eat-3*, suggesting mitochondrial proteotoxicity may be playing a role in arsenite-induced toxicity in fusion-deficient nematodes. Asterisk denotes statistical significance ($p<0.05$) for comparison (one way ANOVA) to untreated control within each strain. N=5–6. Bars±SEM.

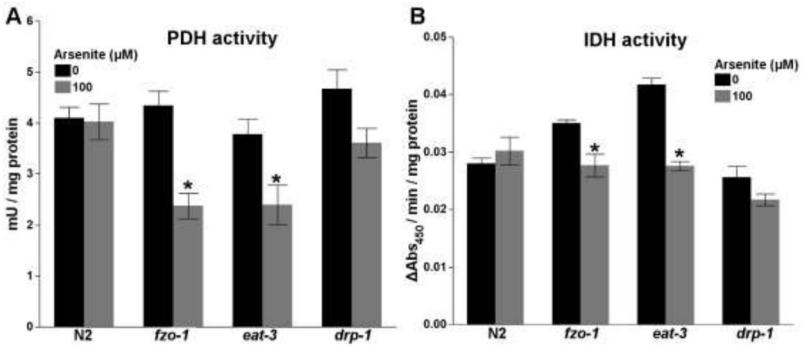

Figure 5. Arsenite inhibits PDH and IDH in *fzo-1*- and *eat-3*-deficient nematodes

24h Exposure to 100μM arsenite in 8-day old nematodes inhibits (A) pyruvate dehydrogenase activity (two way ANOVA, strain ($p=0.0022$), arsenite ($p<0.0001$), interaction ($p=0.041$)) and (B) isocitrate dehydrogenase activity (two way ANOVA, strain, arsenite, interaction ($p<0.0001$ for all)) in *fzo-1*- and *eat-3*-deficient nematodes, suggesting a disruption of pyruvate metabolism and Krebs cycle activity underlie the observed mitochondrial dysfunction in fusion-deficient nematodes. Asterisk denotes statistical significance ($p<0.05$) for comparison (one way ANOVA) to untreated control within each strain. N=6–10. Bars±SEM.

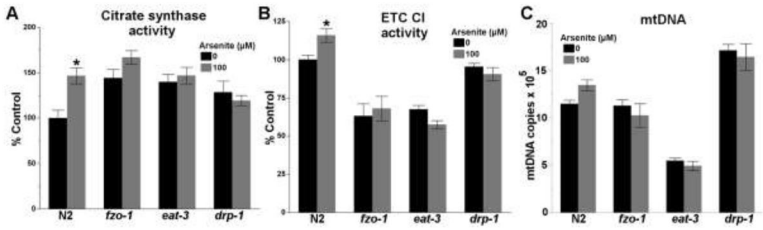

Figure 6. Arsenite increases citrate synthase and ETC CI activity in wild-type nematodes

24h exposure to 100μM arsenite in 8-day old nematodes increased (A) citrate synthase (two way ANOVA, strain (p=0.0029), arsenite (p=0.014), interaction (p=0.030), N=4), and (B) ETC CI activity in wild-type nematodes (two way ANOVA, strain (p=0.66), arsenite (p=0.045), interaction (p=0.030), N=4); however, the apparent trend in (C) increased mtDNA content in wild-type nematodes was not significant (two way ANOVA, strain (p<0.0001), arsenite (p=0.90), interaction (p=0.24), N=6). Asterisk denotes statistical significance (p<0.05) for comparison (Tukeys HSD) to untreated control within each strain. N=5–6. Bars±SEM.

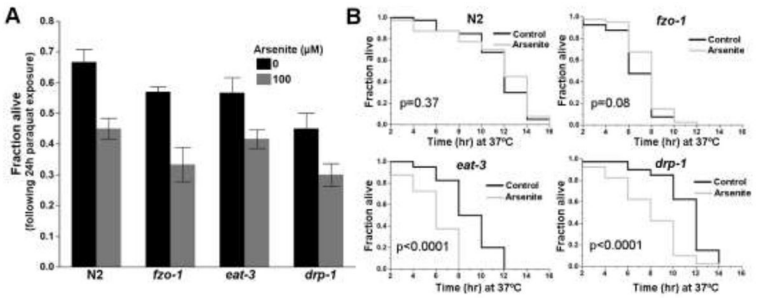

Figure 7. Arsenite sensitizes nematodes to secondary stressors

24h Exposure to 100μM arsenite sensitized nematodes to secondary exposure to the redox cycler (A) paraquat (two way ANOVA, strain ($p=0.0007$), arsenite ($p<0.0001$), but not interaction ($p=0.62$), $n=6$), while only sensitizing *eat-3*- and *drp-1*-deficient nematodes to (B) secondary thermal stress (37°C) (survival curves analyzed via mantel cox test, N=40).

Toxicology. Author manuscript; available in PMC 2018 July 15.

Table 1

Results from toxicant larval growth screen

To summarize the response of each strain to each chemical over multiple doses of each toxicant, data is presented as the average (across doses, as compared to control for each strain) effect of each toxicant on the growth of each nematode strain (percent control ± SEM). In this Table, all statistical comparisons between strains were performed on percent control data, as certain strains grow as reduced rates compared to wild-type (N2) nematodes under control conditions. We first tested whether each toxicant (all doses averaged) had a differential effect on any strain, compared to N2, using a one-way ANOVA (i.e., 1-way ANOVA for all percentage values in each row; p-values reported in toxicant column). All of these were significant; therefore, to determine which strains were different from N2, we carried out post-hoc analysis of each fission, fusion, or mitophagy strain compared to N2 using Dunnett's test (p-values reported in strain columns). While this Table is useful in reasonably accurately presenting a large amount of strain sensitivity data, it does in some cases underreport the biological magnitude of strain effects, because some effects were seen only at some doses, and not at others; and in a few cases, the effect at one dose was opposite that seen at another. In such cases, taking the average values diminished the magnitude of the actual effects. More detailed data can be examined in the Supplemental Figures: Dose-response curves for each strain, shown as ToF (surrogate measure of non-normalized length measurements, allowing a direct comparison of toxicant effect on growth compared to control conditions, within a given strain) and percent growth of control (allowing comparison of between-strain differences) are shown in the indicated supplemental figures

	***C. elegans* strain**					
Toxicant	**N2**	***fzo-1***	***eat-3***	***drp-1***	***pink-1***	***pdr-1***
2,4-DNP Fig S5 (p<0.0001)	96.0 ± 1.1%	83.8 ± 1.3% **(p<0.0001)**	84.3 ± 1.4% **(p<0.0001)**	88.9 ± 1.3% **(p=0.0001)**	87.6 ± 1.4% **(p<0.0001)**	90.0 ± 1.5% **(p=0.003)**
Acetaldehyde Fig S7 (p<0.0001)	77.2 ±0.8%	71.8 ± 0.8% **(p<0.0001)**	70.6.3 ± 0.7% **(p<0.0001)**	76.5 ± 0.7% (p=0.95)	82.0 ± 0.8% **(p<0.0001)**	76.7 ± 0.8% (p=0.99)
Acrolein Fig S8 (p<0.0001)	74.6 ±0.8%	88.1 ± 0.8% **(p<0.0001)**	88.0 ± 0.8% **(p<0.0001)**	80.9 ± 0.8% **(p<0.0001)**	90.0 ± 0.8% **(p<0.0001)**	83.5 ± 0.8% **(p<0.0001)**
Aflatoxin B_1 Fig S2 (p<0.0001)	90.8 ±0.9%	69.1 ± 1.0% **(p<0.0001)**	79.9 ± 0.8% **(p<0.0001)**	87.3 ± 0.9% (p=0.051)	93.5 ± 1.6% (p=0.26)	90.9 ± 1.0% (p=1.00)
Arsenite Fig 1A & Fig S1 (p<0.0001)	90.5 ±0.7%	66.2 ± 0.7% **(p<0.0001)**	65.2 ± 0.7% **(p<0.0001)**	87.4 ± 1.2% (p=0.06)	87.8 ± 1.2% (p=0.10)	93.3 ± 1.1% (p=0.08)
Cadmium Fig S9 (p<0.0001)	44.7 ±0.7%	60.5 ± 0.7% **(p<0.0001)**	49.2 ± 0.7% **(p<0.0001)**	48.8 ± 0.7% **(p<0.0001)**	41.3 ± 0.5% **(p=0.0007)**	44.0 ± 0.6% (p=0.89)
Cisplatin Fig S6 (p<0.0001)	94.6 ±0.7%	65.6 ± 1.7% **(p<0.0001)**	79.9.3 ± 1.3% **(p<0.0001)**	90.9 ± 1.0% **(p=0.04)**	94.3 ± 0.8% (p=0.99)	93.1 ± 0.8% (p=0.72)
Doxycycline Fig S10 (p<0.0001)	75.0 ±1.1%	80.2 ± 1.2% **(p=0.003)**	80.2 ± 1.0% **(p=0.003)**	77.5 ± 1.2% (p=0.33)	68.4 ± 1.0% **(p<0.0001)**	78.2 ± 1.1% (p=0.13)
Paraquat Fig S3 (p<0.0001)	87.6 ±1.0%	78.5 ± 0.9% **(p<0.0001)**	72.1 ± 0.8% **(p<0.0001)**	82.7 ± 0.9% **(p=0.0005)**	84.6 ± 0.8% (p=0.07)	86.1 ± 0.9% (p=0.65)
Rotenone Fig S4 (p<0.0001)	68.0 ±0.8%	53.7 ± 0.7% **(p<0.0001)**	54.3 ± 0.5% **(p<0.0001)**	69.6 ± 0.8% (p=0.31)	50.6 ± 0.6% **(p<0.0001)**	62.3 ± 0.7% **(p<0.0001)**

Table 2

24h arsenite LC_{50} values with 95% confidence intervals in parentheses

Strain	LC_{50} (mM) at L4 stage (95% C.I.)	LC_{50} (mM) at day 8 (95% C.I.)	LC_{50} (mM) at day 12 (95% C.I.)
N2	5.73 (2.93 – 8.52)	1.81 (1.06 – 2.57)	0.64 (0.45 – 0.84)
fzo-1	2.76 (2139 – 3376)	0.91 (0.66 – 1.16)	0.22 (0.10 – 0.35)
eat-3	2.97 (2.15 – 3.80)	0.38 (0.22 – 0.53)	0.12 (0.71 – 0.17)
drp-1	6.03 (2.42 – 9.64)	0.97 (0.69 – 1.26)	0.38 (0.23 – 0.54)